Peer-reviewed version available at *Water* **2020**, *12*, 1291; doi:10.3390/w12051291

Article

Sources of salinization of groundwater in the Lower Yarmouk Gorge, East of the River Jordan

Peter Möller [1,*], Marco De Lucia[1], Eliahu Rosenthal[2], Nimrod Inbar[3,4], Elias Salameh[5], Fabien Magri[6,7], Christian Siebert[8]

1 GFZ German Research Centre for Geosciences, Potsdam, Germany
2 The School of Earth Sciences, Tel Aviv University, Tel Aviv, Israel
3 Department of Geophysics and Space Sciences, Eastern R&D, Ariel, Israel
4 Department of Physics, Ariel University, Ariel, Israel
5 University of Jordan, Amman, Jordan
6 BfE Federal Office for the Safety of Nuclear Waste Management, Dept. FA 2, Berlin, Germany
7 Free University of Berlin, Hydrogeology, Berlin, Germany
8 Helmholtz Centre for Environmental Research UFZ, Dept. of Catchment Hydrology, Halle, Germany
* Correspondence: pemoe@gfz-potsdam.de

Abstract: In the Lower Yarmouk Gorge the chemical composition of regional, fresh to brackish, mostly thermal groundwater reveal a zonation in respect to salinization and geochemical evolution, which is seemingly controlled by the Lower Yarmouk fault (LYF) but does not strictly follow the morphological Yarmouk Gorge. South of LYF the artesian Mukeihbeh well field produces in its central segment groundwaters of almost pure basaltic-rock type with low contribution (< 0.3 vol-%) of Tertiary brine, hosted in deep Cretaceous and Jurassic formations. Further distal, the contribution of limestone water increases originating from the Ajloun Mts. North of the LYF, the Mezar wells, the springs of Hammat Gader and Ain Himma produce dominantly limestone water, which contains 0.14-3 vol-% of the Tertiary brine and possess hence variable salinity. The total dissolved equivalents of solutes gained by water/rock interaction (WRI) and mixing with brine, $TDE_{WRI+brine}$, amounts to 10-70 % in the region comprising the Mukheibeh field, Ain Himma and Mezar 3 well, to 55-70 % in the springs of Hammat Gader, and to 80-90 % in wells Mezar 1 and 2. The type of salinization indicates that the Lower Yarmouk fault seemingly acts as the divide between the Ajloun and the Golan Heigths dominated groundwater.

Keywords: Hauran Plateau; Golan Heights; Ajloun Dome; Yarmouk basin; Salinization; Mixing of water types; Statistical modelling

1. Introduction

The study of the hydrochemical compositions of groundwater and brines reveals the origin of water and its salinization (e.g. [3,8,14–16,18,20,29,48,50–52]). The inorganic composition of groundwater depends on weathering of minerals in the catchment rocks, water/rock interaction (WRI) along the flow paths and the amounts of atmospheric deposition [62]. The processes together yield typical ionic ratios in groundwater ([26] and references therein).

Contrasting the behaviour of major elements in groundwater, trace elements such as the rare earth elements (REE) and uranium behave differently [52]. Their extremely low concentrations (<μmol/l) are controlled by adsorption onto mineral surfaces and co-precipitation with alteration minerals [4,34,35,55–60]. Among the trace elements the suite of REE and Y (henceforth combined to REY) is a well-known tool in identification of the origin of groundwaters [14–16,20,29,52,53]. REY immediately

achieve steady state conditions in the infiltrating water due to their high charge and affinity to build surface complexes. For instance, more than 99 % of REY released from dissolving calcite in limestones is immediately adsorbed onto calcite surfaces [26]. During migration of groundwater REY are continuously subjected to exchange with surface-adsorbed REY. Thus, after some time the REY patterns of groundwater resemble those gained during weathering of the catchment rocks [26]. Therefore, REY patterns characterise the lithology of the recharge area, whereas major and minor elements reflect the solubility of minerals of the entire assemblage of catchment and aquifer rocks. The conjoint application of major and trace elements in the water yield the necessary deep insight into its salinization and flow paths [43,51–53].

This study aims at the identification of groundwater sources and their salinization in different geological formations in the productive region of the Lower Yarmouk Gorge (LYG) shared by Israel, Jordan and Syria. Particularly the issue of potential transboundary flow of water between the Ajloun in the south [46,47] and the Golan Heights in the north [10,41,44,51] underneath the Yarmouk River was and still is debated. It has been considered whether or not the Gorge delineates a fault or represents an anisotropy zone which possibly prevents transboundary flow of groundwater between Jordan and Israel [12,61]. Seismic lines crossing this border have not been shot up to now but several ones in the southern Golan Heights [13]. Shallow faults in northwest Jordan are described in [45]. Based on these surveys and additional evidences [13] suggest a strike-slip-flower-structured fault system and numerous buried faults crossing the Gorge acute-angled (Fig. 1). The productive water resource in the LYG is vitally important for Jordan and Israel because of shortness of water in both countries [40]. Like elsewhere in all semi-arid regions in the world, the ground- and surface water resources are over-exploited leading to suffering from water shortness due to increasing demand and the consequences of climate change [51]. In such regions water supply is a serious socio-economic and political issue, if transboundary flow is involved. For sustainable management and protection of groundwater resources, water authorities need detailed knowledge of (i) the respective recharge area of distinct wells or well fields, (ii) the flow characteristics and (iii) possible inter-aquifer flow [7]. In areas with transboundary water resources also rules of equitability and no-harm have to be obeyed in order to prevent political interferences [6].

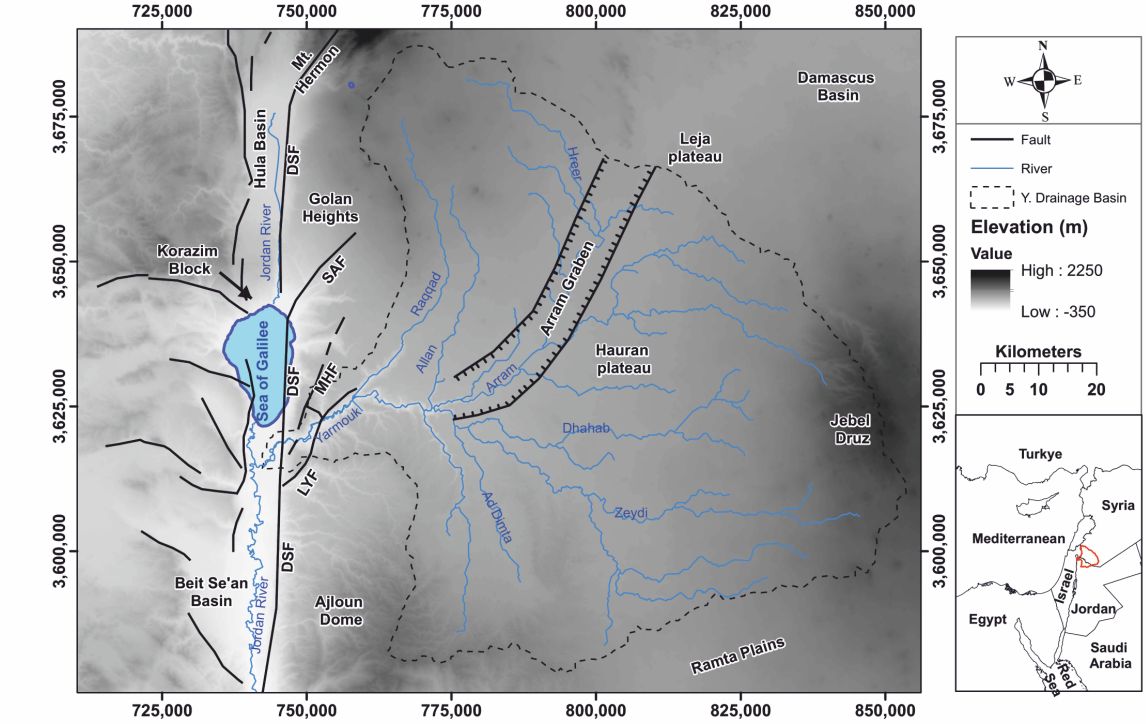

Figure 1. Overview of the Yarmouk drainage basin and its environment. The basin is outlined in red in the lower insert. Note the graben structure with the perennial Arram River in the Yarmouk basin. DSF=Dead Sea Transform fault; SAF=Sheikh Ali fault; MHF=Mevo Hamma fault; LYF=Lower Yarmouk fault.

2. Hydrogeological setting

The Yarmouk basin comprises the eastern Golan Heights and south-eastern flanks of the Hermon Massif, shared by Israel and Syria, the northern plunges of the Ajloun Dome (Jordan), and the Hauran Plateau including the western flank of the Jebel Druz (Syria) (Fig.1). The LYG is the major outlet of surface and groundwater from the Yarmouk basin. Morphologically, the Gorge separates the Ajloun Mountains and the Jordanian Ramta Plains from the Golan Heights and the Hauran Plateau, respectively.

The anticlinal structure of the Ajloun is built of Lower Cretaceous Kurnub sandstones and Upper Cretaceous, marine, strongly karstified, fractured and silicified lime- and dolostones forming the *A7/B2* aquifer in Jordan (Fig.2), which descends northward. For easement and shortness, the Jordanian nomenclature of formations is preferred in this contribution. Groundwaters in the *A7/B2* are confined by the overlying bituminous Senonian *B3* aquiclude, which contains phosphorite, chert and chalk and separates the *A7/B2* from the locally exploited limy *B4* aquifer.

Age		Group		Formation		Hydrogeological properties	
Period	**Epoch/Stage**	**Golan**	**Ajloun**	**Golan**	**Ajloun**	**Golan**	**Ajloun**
Quaternary	Holo-/Pleistocene			Yarmouk Basalt			basalt
Neogene	Pliocene	Kefar Giladi	Belqa	Cover Basalt			basalt
				Bira/Gesher			silicified limest., dolomite
	Miocene			Hordos	Waqqas Conglomerate (WC) - Jordan Valley		marl, sand
				Lower Basalt			alkali olivine basalt
Paleogene	Oligocene			Susita/Fiq			marlst., sandy dolomite
	Eocene				**B5** Wadi Shallalah Chalk (WSC)		chalk, bituminous
		Avedat		Maresha/Adulam	**B4** Umm Rijam (URC)	marl, chalk, limestone	chalky limest., chert beds
Upper Cretaceous	Upper Maastricht-Paleocene	Mt. Scopus		Taqiye	**B3** Muwaqqar Chalk (MCM)	bituminous, chert, phosphorite	micritic limest., bituminous (oilshale)
	Masstrichtian			Ghareb	**B2b** Al Hasa Phosphorite (AHP)		calcareous, phosphorite beds, limest., chalk, marl
	Campanian			Mishash	**B2a** Amman silicified limestone (ASL)	marly limestone,	limest., chalky dolomite, phosphate, chert
	Santonian			Menuha	**B1** Wadi Umm Ghudran (WUG)		massive chalk, limest., phosphatic sandst., chert
	Turonian	Judea	Ajloun	Bina	**A7** Wadi Es Sir Limest. (WSL)	limestone, dolomite, marly limest.	dolomitic limest., sandst., cherts
	Cenomanian-Turonian				F/H/S-undifferentiated		marl and gypsum
					A5-6 Shueib (S)		siltstone, marly limest., dolomite
Period	**Epoch/Stage**	**Hermon**	**Ajloun**	**Hermon**	**Ajloun**	**Hermon**	**Ajloun**
Upper Jurrassic	Tithonian Kimmeridgian	Arad	Zarqa	J6-J7 (Nahal Saar)	Azab	limestone	sandstone, siltstone, limestones
	Oxfordian			J5 (Kidod)		marl, shale	
Middle Jurassic	Aalenian-Callovian			J4 (Hermon/Zohar)		limestone	
Lower Jurassic	Hettangian-Toarcian			J1-J3		dolomite, limestone	

Figure 2. Stratigraphic table comparing the Israeli and Jordanian nomenclature. Aquiferous units are colored in blue after [52].

The Cretaceous and Tertiary sedimentary aquifers, which crop out in the Ajloun anticline descend northward into the Golan syncline and surface later again at the foothills of the Hermon anticline, which consists of thick Jurassic lime- and dolostone aquifers with abundant basaltic intrusions [49]. As a consequence, groundwaters south and north of the Gorge migrate through the same aquiferous formations. Contrasting the Ajloun, the Golan Heights are unconformably covered by up to 700 m thick Plio-Pleistocene Cover Basalt [33,39]. A marly sequence at its base, the highly fractured basalt serves as a regional aquifer being annually directly recharged by 500-1,200 mm of precipitation [8]. During the pre-Quaternary the Golan Heights were subjected to tectonic stress documented in a highly faulted and deformed subsurface [24] with intense and deep karstification of the Upper Cretaceous and Tertiary lime- and dolostones [11]. A meridional ridge in these formations acts as subsurface water divide in the covering basalt aquifer [8], leading to groundwater drainage in the latter either W-SW to the Hula- and the Sea of Galilee basin or E-SE into the Hauran Plateau and the Upper Yarmouk Gorge. Hydraulic connections between the basaltic cover and the underlying aquiferous Cretaceous carbonate formations may exist throughout the Golan Heights [25].

The eastward continuation of the Golan Heights is the flat and southward dipping volcanic area of the Hauran Plateau, which passes in the SE into the enormous accumulation of Neogene-Quaternary basalts of the Jebel Druze [17,22]. Precipitation infiltrates directly into Upper Quaternary basalts exposed all over the Plateau and drains towards the LYG, partially feeding perennial springs in the arcuated Wadi Arram (Fig. 1) which was a major contributor to the Yarmouk River in the past [9].

Along the northern flank of the LYG, hot groundwater emerges at Hammat Gader springs (codes EM, ER and EB in Table 1; 38-43 °C) from the *B3* aquitard (Arad and Bein 1986) and ascend with 41-60 °C in the artesian wells of Mezar from *A7* (Mezar 2) and *B2* (Mezar 3) aquifers (Fig. 3).

Table 1. Analyses of spring and well waters from the Lower Yarmouk Gorge. Grouping according the geographical and chemical proximity (code). In the two last columns the normalized Tb/Lu ratios and the fraction of basaltic-rock water, bw, in mixture with limestone water are given as derived from Fig. 4.

Code	Source	Samp.	Xing	Ying	pH	Eh	Temp	EC	Alk	Ca^{2+}	Mg^{2+}	K^{+}	Na^{+}	Cl^{-}	SO_4^{2-}	HCO_3^{-}	TDE
Group		Date				mV	°C	μS/cm	mg/l	meq/l							
U-1	Mukheibeh 2	2016	753241.00	3622342.00	6.13	17.90	28.90	830.00	4.56	3.90	2.14	0.07	1.70	1.59	1.17	4.50	15.07
U-1	Mukheibeh 4	2016	753212.00	3622331.00	7.04	272.71	29.10	827.00	4.76	4.20	2.30	0.07	1.74	1.59	1.19	4.69	15.79
U-1	Mukheibeh 4	2013	753209.00	3622333.00	7.10	62.99	28.80	807.00	5.18	4.80	2.39	0.08	1.67	1.56	1.14	5.11	16.75
U-1	Mukheibeh 2	2013	753243.00	3622340.00	7.12	64.61	28.14	809.00	5.18	4.80	2.47	0.08	1.68	1.65	1.19	5.11	16.98
U-1	Mukheibeh 1	2001	753119.09	3622153.88	7.00	66.71	29.10	797.00	5.93	4.57	2.47	0.08	1.70	1.61	1.13	5.86	17.42
U-2	Mukheibeh 6	2016	753018.00	3622417.00	7.06	-40.08	31.00	667.00	5.08	4.30	2.39	0.09	2.13	2.07	1.25	5.01	17.23
U-2	Mukheibeh 7	2016	754257.00	3623142.00	7.17	-17.13	38.50	774.00	4.80	4.20	2.39	0.07	1.74	1.71	0.74	4.73	15.57
U-3	Mukheibeh 10	2016	753267.00	3622856.00	6.96	-116.60	39.00	710.00	4.34	3.60	2.06	0.09	2.04	1.69	0.82	4.27	14.58
U-3	Mukheibeh 5	2016	747753.00	3618570.00	7.32	161.62	40.90	876.00	5.08	3.55	1.98	0.10	2.04	1.61	0.76	5.00	15.04
U-3	Mukheibeh 11	2016	753845.00	3622588.00	6.92	200.18	31.90	821.00	4.80	3.80	3.21	0.07	1.91	1.59	1.11	4.73	16.43
U-3	Mukheibeh 9	2016	756312.00	3624296.00	7.20	-67.10	28.90	1157.00	7.60	2.70	2.39	0.41	5.22	2.33	0.44	7.52	21.00
U-3	Mukheibeh 8	2013	755490.00	3624127.00	7.45	-123.14	44.90	701.00	4.72	3.40	1.65	0.13	2.32	1.82	0.58	4.64	14.53
U-3	Mukheibeh 8	2016	755495.00	3624134.00	7.16	-62.14	44.90	723.00	4.10	2.95	1.65	0.13	2.43	1.88	0.26	4.03	13.33
U-3	Mukheibeh 13	2016	754268.00	3623212.00	7.12	-46.50	38.90	778.00	4.40	3.60	2.06	0.09	2.00	1.74	0.71	4.33	14.53
U-3	Mukheibeh 13	2013	754280.00	3623202.00	7.38	-76.13	38.50	752.00	5.12	4.05	2.06	0.10	1.90	1.67	0.51	5.04	15.32
ES	Ein Sahina	2016	750190.00	3619926.00	7.04	453.74	28.00	844.00	5.00	4.35	2.30	0.08	1.91	1.88	1.02	4.93	16.48
AH	Ein Himma	2007	751665.20	3621722.40	7.02	-27.54	40.00	1433.00		5.67	2.80	0.35	5.31	6.88	4.43	6.88	32.32
AH	Ein Himma	2001	751665.20	3621722.40	7.06	-144.95	41.50	1418.00	5.59	5.38	2.87	0.36	5.40	5.86	3.09	5.52	28.47
AH	Ein Himma	2013	751600.00	3621710.00	7.10	71.63	37.70	1130.00	4.84	5.90	2.63	0.23	3.67	4.23	2.60	4.77	24.04
AH	Ein Himma	2016	751661.00	3621700.00	7.03	85.46	40.00	499.00	4.06	5.50	2.47	0.24	4.09	4.54	2.69	4.00	23.53
AS	Ain Saraya	2016	750429.00	3619424.00	6.83	-15.94	38.30	1655.00	4.54	6.50	3.13	0.31	6.96	9.65	2.50	4.47	33.51
ER	Ein Balsam	2016	749705.00	3619324.00	6.76	10.68	41.90	1600.00	4.80	6.00	2.80	0.31	5.65	9.17	2.77	4.73	31.43
ER	Ein Reach	2016	750014.00	3619198.00	6.69	-75.73	43.40	1860.00	4.84	6.50	3.05	0.36	6.96	10.61	2.67	4.78	34.91
ER	Ein Reach	2000	750348.73	3619398.73	6.85	-95.66	38.00	1728.00	6.00	7.12	3.25	0.31	6.23	8.71	2.39	5.93	33.95
ER	Ein Reach	2004	749984.63	3618815.84	6.81	-146.95	41.50	1759.00	5.86	6.72	3.25	0.32	6.79	9.75	2.48	5.79	35.11
EM	Ein Makla	2016	749859.00	3619141.00	6.59	-116.47	49.50	2160.00	3.64	7.50	3.21	0.44	9.13	13.40	3.12	3.58	40.38
EM	Ein Makla	2000	749908.86	3619091.42	6.64	-131.40	47.30	2190.00	5.64	8.91	3.64	0.46	9.23	13.77	3.30	5.57	44.88
EM	Ein Makla	2004	749811.00	3618793.22	6.73	-166.56	49.60	2160.00	5.42	7.58	3.46	0.44	9.12	13.13	3.14	5.35	42.23
ME1	Meizar 1	2016	752652.00	3625884.00	7.38	-79.02	35.20	1630.00	3.64	2.60	1.40	0.33	10.00	10.89	0.26	3.56	29.05
ME2	Meizar 2	2016	752706.00	3622894.00	6.40	-76.90	60.60	2080.00	3.68	8.50	3.05	0.62	9.13	11.06	7.04	3.62	43.01
ME2	Meizar 2	2001	752700.04	3622913.60	6.63	-102.33	60.00	1650.00	4.06	7.12	2.86	0.56	7.74	8.93	5.80	4.00	37.01
ME3	Meizar 3	2016	752725.00	3622926.00	6.81	-119.60	42.20	810.00	5.48	3.55	2.06	0.10	2.30	2.22	0.40	5.41	16.05
ME3	Meizar 3	2001	752706.85	3622922.74	7.09	-129.23	41.80	664.00	5.24	3.27	1.72	0.12	2.11	1.74	0.08	5.17	14.20
YR	Yarmouk	2016	756255.00	3624301.00	8.40	190.97	23.50	961.00	3.18	2.75	2.47	0.15	4.22	3.10	3.06	3.02	18.77

South of the Yarmouk River the hot water from Ain (Arabic term for spring) Himma (42 °C) emerges from the *B3* aquitard, ascending along faults from the *B2* aquifer [3]. In the nearby artesian Mukheibeh well field the groundwater is exploited from *A7* and *B2* discharging with temperatures of 29-46 °C probably heated by volcanic intrusions at depths of 3-4 km [36]. Hot groundwater from the *A7* aquifer is also known from the western Ajloun escarpment within the Lower Jordan Valley [27,28,46]. In the Ajloun the temperature of groundwater from *A7/B2* is only slightly enhanced (23-31 °C) and cool if draining the shallow basaltic aquifer or the *B4*.

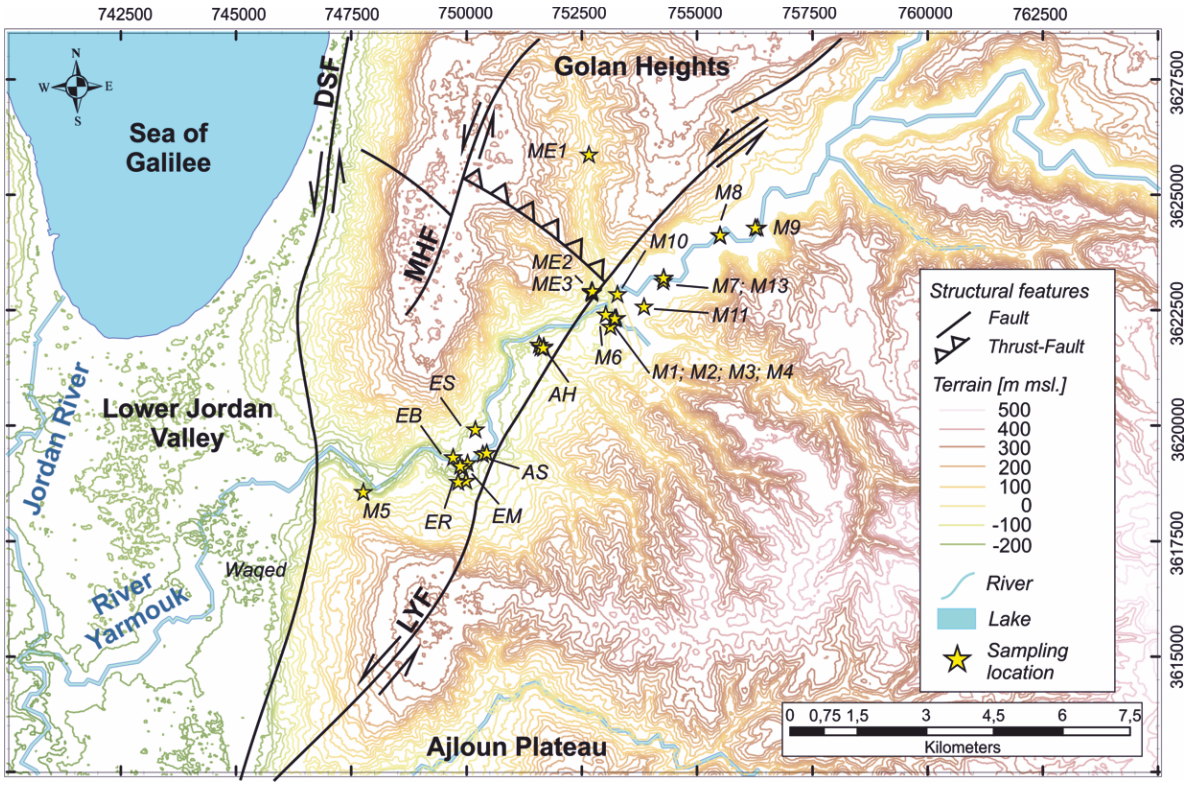

Figure 3. A detailed view of the sampling locations in the Lower Yarmouk Gorge. Very important are the Lower Yarmouk (LYF)- and Mevo Hamma faults (MHF) and the rise of the Hammat Gader block in between. DST= Dead Sea Fault. The region of Hammat Gader encloses codes, EB, ER and EM (Table 1).

With few exceptions the groundwater of the LYG are saturated with respect to calcite but neither to gypsum nor halite [51]. The groundwater from Ain Himma, the springs of Hammat Gader (enclosing codes ES, EB, ER and EM in Table 1) and Mezar well 3 are seemingly mixtures of local groundwater, relic seawater evaporation brine(s) and leached evaporites and dissolved calcite from limestone [51,52].

3. Materials and methods

3.1. Sampling and analytical procedure

During a synchronous sampling campaign in 2016, wells and springs on both sides of the LYG were chemically analyzed. To allow a regionally comprehensive elaboration, selected analytical results from earlier local campaigns were included (Table 1). In the field, samples were collected by filtrating (0.22 µm) water into cleaned HD-PE bottles. Cation samples have been acidified to ensure conservation. To determine REY and U(VI), preconcentration was required. Therefore, about 4 l of sample were filtered (0.22 µm), acidified by sub-boiled (index sbb) HCl to a pH=2, and spiked with 1 ml of Tm solution. At the same day, the samples were passed through C_{18} Sep-Pak cartridges, loaded with ethylhexylphosphate liquid ion exchanger. In the lab, each cartridge was eluated with HCl_{sbb} and eluates were evaporated to incipient dryness, taken up with HNO_{3sbb} and the resulting solution was

analyzed applying ICP-MS (Elan DRC-e). Independently, Ca^{2+} and Mg^{2+} were determined by similar ICP-MS. K^+ and Na^+ were analyzed by ICP-AES (Spectro Arcos) using matrix adjusted standard solution for calibration. Cl^-, Br^-, SO_4^{2-} were determined by Dionex ICS (AS18 column). The alkalinity was titrated to pH 4.3 with H_2SO_4 and given as HCO_3^-.

3.2. Selection of end member fluids in the Yarmouk basin

The suggested quantification of salinity contributions is based on defined end members of water types in the LYG:

- Infiltration of precipitation over basaltic catchments, particular in the Hauran plateau;
- Infiltration of precipitation over limestones catchment mainly in the Ajloun Mts. and Mt. Hermon /Golan Heights;
- Relics of brines residing in Jurassic-Cretaceous limestones, and
- Dissolution of evaporites and water/rock interaction (WRI) along flow paths.

Basaltic-rock- and limestone waters with lowest Cl^- concentrations are suggested as end members because enhanced Cl^- concentrations suggest dissolution of halite from evaporites and/or leaching of seawater brines enclosed in limestones. The lowest Cl^- concentrations of basaltic-rock water from the Golan and Hauran Plateau are 0.46 and 0.32 meq/l, respectively (Table A1 and Table 1).

The averages of limestone water of two well waters from each the Golan Heights and the Ajloun Mts. were selected. Their Cl^- concentrations range between 0.50 and 0.80 meq/l (Table 2). This wide spread suggests that the samples with values >0.50 meq/l might have already leached either evaporites or contain seawater brines.

Table 2. Averages of water types in the Lower Yarmouk Gorge. For more details refer to appendix.

	Ca^{2+}	Mg^{2+}	K^+	Na^+	Cl^-	SO_4^{2-}	HCO_3^-
	meq/l						
Basaltic-rock water	1.218	0.720	1.049	0.069	0.393	0.174	2.290
Ajloun limestone water	4.93	1.02	0.04	0.712	0.80	0.22	4.66
Golan limestone water	0.388	0.493	0.101	2.164	0.502	0.100	2.10
Ha'On brine	45.10	123.4	8.79	254.9	421.0	4.31	8.42
Rosh Pinna brine, 2486-2586 m	239.7	59.62	9.18	348.0	642.8	24.19	6.06

Two particular brines have to be considered:

1. The Late Tertiary brine was generated by evaporation of intruded Tethys seawater into the Jordan-Dead Sea Rift [31]. This evaporation brine infiltrated the Cretaceous and Jurassic aquifers east and west of the Rift. This type of Mg^{2+}-Cl^- brine was identified at Ha'On in the 1960s [21] along the SE shore of Lake Tiberias. The variations in composition of two wells at Ha'On between 1961 and 2004 are averaged (Table 2). For more detail refer to Table A1.
2. The Late Triassic- to Early Jurassic brine of Rosh Pinna is hosted at depths of 2,500 m in limestones of the Korazim block north of Lake Tiberias (Fig. 1). This brine represents a mixture with the Tertiary Ha'On of brine and fresh water [42].

3.3. Estimation of fractions of brine, basaltic-rock- and limestone water

The fractions of basaltic-rock water, ε_{bw}, in mixtures of both pure basaltic-rock water and limestone water (Fig. 4a), are derived from interpretation of REY distribution patterns showing the variation of mixtures of both types of groundwater. Each of the REY patterns is characterized by C1 chondrite-normalized Tb/Lu values [1] that decrease with increasing ε_{bw} values (Fig. 4b), which is used to approach reliable ε_{bw} for the corresponding Tb/Lu values of each groundwater in the study area. For more information of REY patterns refer to [52]. This approach of ε_{bw} assumes that

the REY patterns are not significantly varied by dissolution of evaporites or by WRI. Applying ε_{bw} and $\varepsilon_{lmst} = 1 - \varepsilon_{bw}$, the end member composition of basaltic-rock- and limestone water (Table 2) and the analysed concentrations of species i, $c_{i,agw}$ in Eq. 1 yields the sum of $\varepsilon_{brine} \cdot c_{i,brine} + c_{i,WRI}$ of each species i. The summation of contribution of Cl^- from basaltic-rock- and limestone water is given as "estimated" $c_{Cl,est}$ by Eq. 2. If halite is absent, the maximum fraction of ε_{brine} is derived from Eq. 3 which probably yields an overestimation.

$$c_{i,agw} = \varepsilon_{bw} \cdot c_{i,bw} + (1 - \varepsilon_{lmst}) \cdot c_{i,bw} + \varepsilon_{brine} \cdot c_{i,brine} + c_{i,WRI} \quad (1)$$

$$\varepsilon_{bw} \cdot c_{Cl,bw} + (1 - \varepsilon_{lmst}) \cdot c_{Cl,bw} = c_{Cl,est} \quad (2)$$

$$c_{Cl,agw} - c_{Cl,est} - \varepsilon_{brine} \cdot c_{Cl,brine} = 0 \quad (3)$$

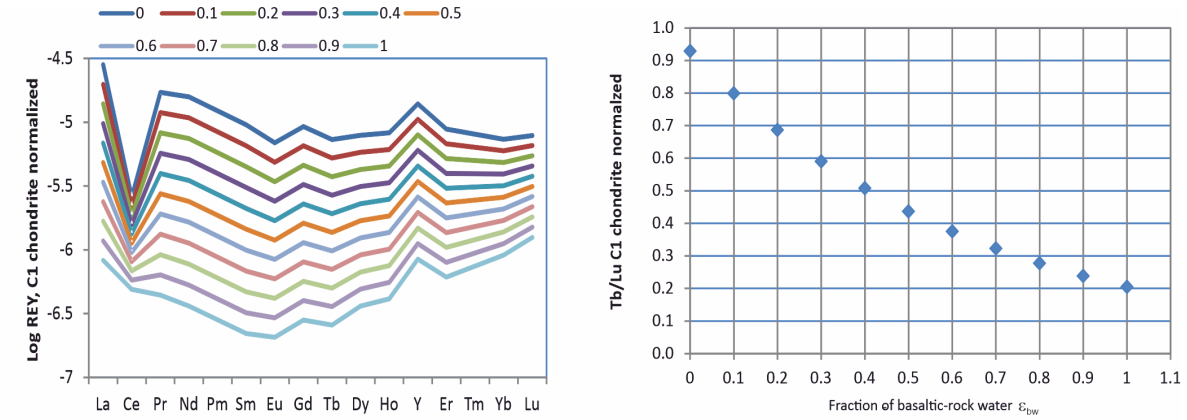

Figure 4. Variation of rare earth element distribution patterns in mixtures of basaltic-rock- and limestone water. (a) Estimates of mixing of basaltic-rock-(1) and limestone water (0); (b) resulting C1 chondrite normalized Tb/Lu values as function of ε_{bw}. REY data are taken from [52] and are normalized to C1 chondrite to get smooth curves. The average of Ein Dan and Ein Banyas in Mt Hermon Massif are used as pure limestone water; as basaltic-rock water the analysis of Mukheibeh 2/2013 is used. Data are taken from [51].

Another way to characterize the salinization of groundwater is achieved by estimating the total dissolved equivalents TDE (in meq/l), which is independent on processes by such as ion exchange with clay minerals, albitization, dolomitization. TDE, however, varies due to dissolution and precipitation of minerals and mixing of fresh and saline waters. TDE_{bw} and TDE_{lmst} are estimated for the contributions of corresponding waters (Eq. 4). TDE of the analyzed groundwater, TDE_{agw}, is given by summation over all dissolved species i (Eq. 5). The sum of TDE_{WRI}+TDE_{brine} is estimated according to Eq. 6.

$$TDE_{est} = TDE_{bw} + TDE_{lmst} \quad (4)$$

$$TDE_{agw} = TDE_{est} + TDE_{brine} + TDE_{WRI} \quad (5)$$

$$\Sigma \left[c_{i,agw} - (\varepsilon_{bw} \cdot c_{i,bw} + (1 - \varepsilon_{bw}) \cdot c_{i,lmst}) \right] = TDE_{WRI} + TDE_{brine} = TDE_{WRI+brine} \quad (6)$$

4. Results

4.1. Correlations of solutes in Yarmouk groundwater

The cross plots of dissolved species in groundwater reveal relationships between end members of saline and fresh water. The fresh water end member of basaltic-rock- and limestone water (Table 2) are implemented in Fig. 5. The correlation of various elements with Cl^- reveals several aspects: Mukheibeh concentrations either tightly cluster (Figs. 5a-d) or spread in one direction (Figs. 5e-f). Waters from Hammat Gader and Mezar/Himma seem to represent dilution lines with different saline end members and the assumed basaltic-rock- and limestone water both plotting near the Mukheibeh cluster. The same may be true for Fig. 5d, where the Br^- concentrations of the low-salinity end members are close to zero. Values of Ca^{2+} and Mg^{2+} in fresh water show a wide spread with diverging (Fig. 5e) or monotonous (Fig. 5f) increase with increasing Cl^-. The Mukheibeh waters show enhanced Ca^{2+} and Mg^{2+} concentrations compared with the basaltic rock water and limestone water.

Preprints (www.preprints.org) | NOT PEER-REVIEWED | Posted: 28 February 2020 doi:10.20944/preprints202002.0414.v1

Peer-reviewed version available at Water 2020, 12, 1291; doi:10.3390/w12051291

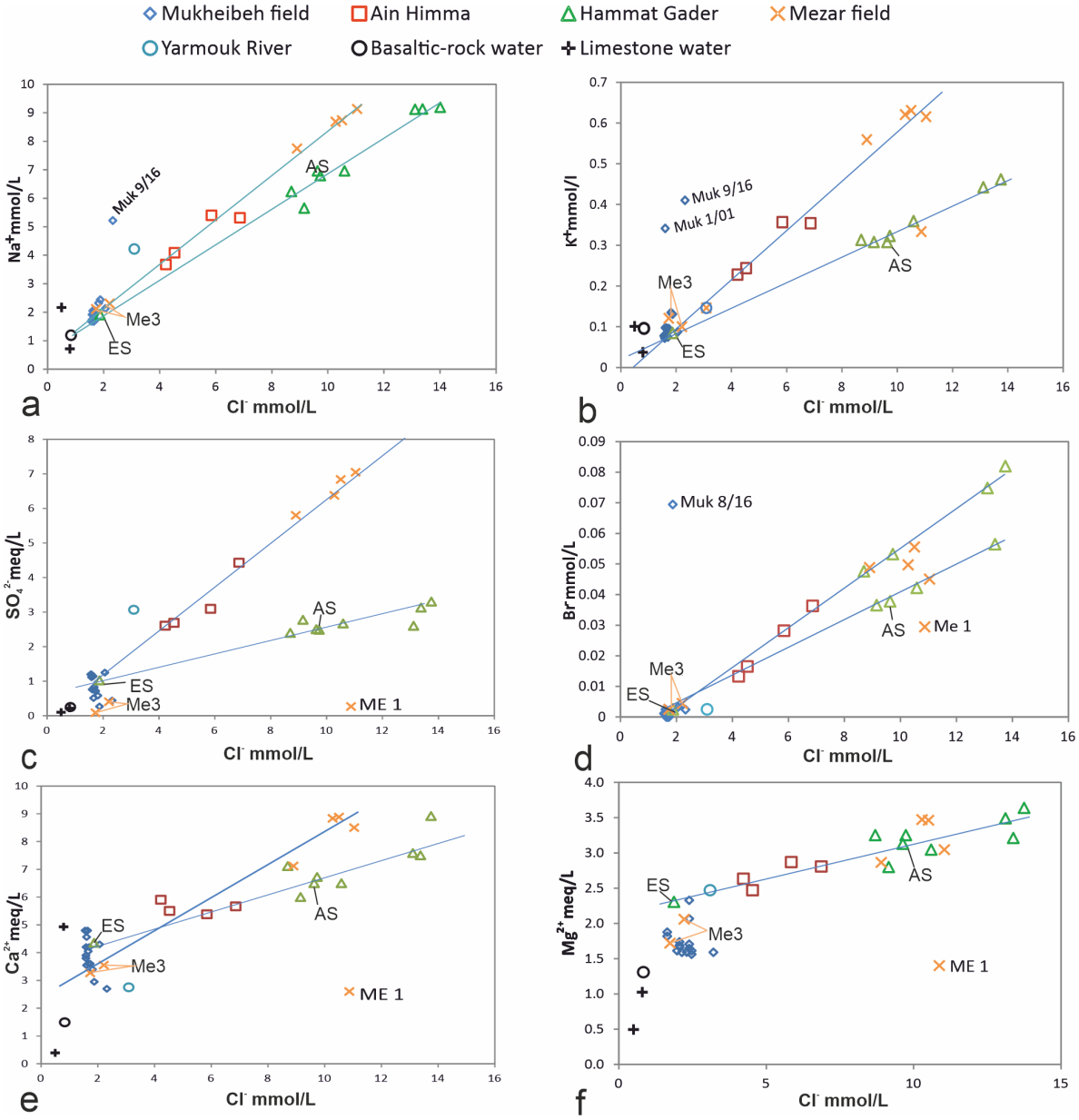

Figure 5. Cross plots of dissolved species in groundwater. Note that the high-salinity groundwaters are related to either basaltic or limestone water (a-e). This is not the case in (f). Averages of low Cl^- containing water from the Ajloun Mts. and from the Golan Heights are used for limestone water. Average of low Cl^- containing water from the Hauran Plateau are used for basaltic-rock water (Table 1). x/yy indicates the sampling ID and the year of sampling in the 21th century.

More details reveal the indicated trend lines in the cross plots of $1000 \cdot Br^-/Cl^-$ and Na^+/Cl^- (Fig. 6). For orientation the trend of evaporated seawater is given as red line [23,37]. The groundwater from springs of Hammat Gader and Himma and from well Mezar 2 define vertical trends, which are only explainable by leaching of Br^- from the organic-rich limestones of the *B3* aquitard. Mezar 1 and 3 and the low Br^-/Cl^- samples of all vertical trends suggest a mixing line between Mukheibeh groundwater and evaporated seawater such as the Ha'On brine [32]. A second mixing line is indicated by Ein (Hebrew term for spring) Sahina (ES) and the wells Mukheibeh 1 and 6. The water of Mukheibeh 9 well shows an extreme position.

Preprints (www.preprints.org) | NOT PEER-REVIEWED | Posted: 28 February 2020 doi:10.20944/preprints202002.0414.v1

Peer-reviewed version available at Water 2020, 12, 1291; doi:10.3390/w12051291

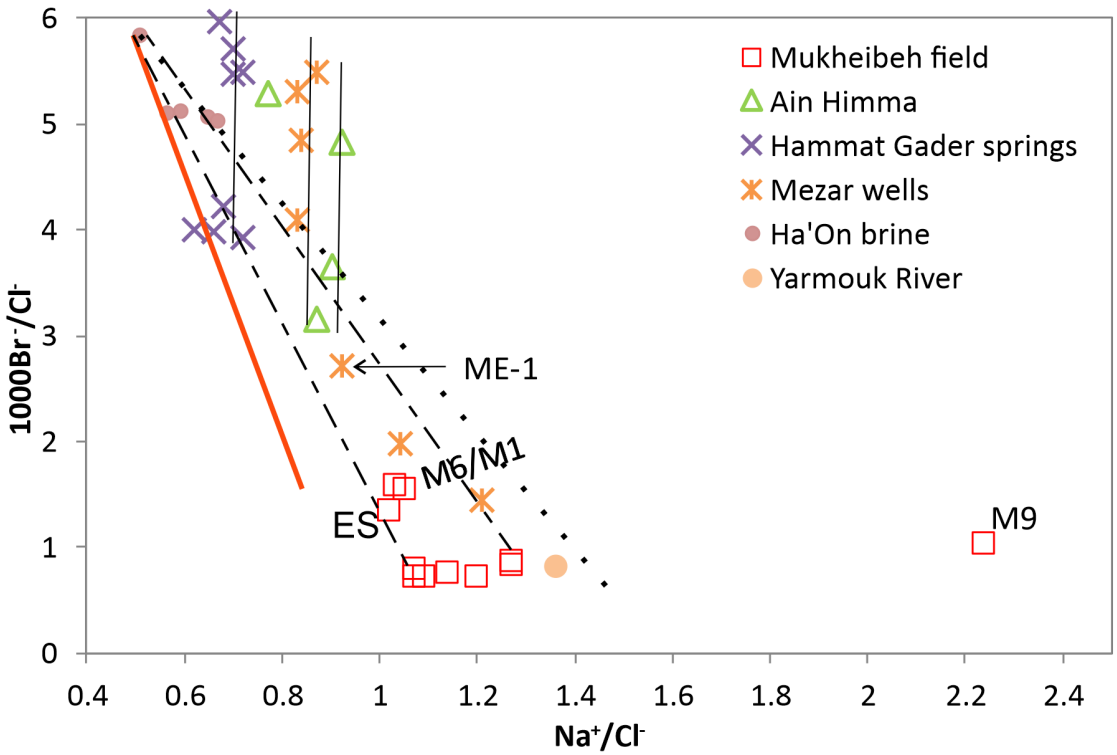

Figure 6. Cross plots of Na^+/Cl^- vs $1000 \cdot Br^-/Cl^-$ of Ha'On brine analyses in the years 1961 to 2004 and of evaporated seawater (red line) [23,37]. Present-day Ha'On brine is a dilution product of the original Ha'On brine and basaltic-rock groundwater with $Na^+/Cl^- > 1$ (dashed line). The intersection of the dilution line with the trend line of evaporated seawater approach the values of Na^+/Cl^- and $1000Br^-/Cl^-$ of the original Tortonian Ha'On brine to be 0.43 and 5.9, which significantly deviate from the measured ones in the years of 1961 and 2004 (Table 1). The vertical lines indicate leaching of Br^- from *B2*. The solid line represents mixing of Ha'On brine and basaltic-rock water in the Mukheibeh field. M= Mukheibeh sample.

Applying the partitioning around medoids clustering method [38] on the groundwaters of the LYG, using the L1 norm for distance measure (=sum of the absolute distances of all components) (Fig. 7), identifies the same distinct clusters ("code" in Table 1) based only on geographical and chemical proximity. The results of this analysis are visualized in terms of three principal components, which cumulatively explain 83 % of the variance of the samples. The spheres in Fig. 7 represent the position of samples in the vectorial space of the principal components; the similarly colored small dots indicate the corresponding projections on the three faces of the cube. In the C1/C2 plane Mukheibeh waters (code U1, U2, U3 in Table 1) yield a curve which is far away from the projection of Hammat Gader samples (codes ER and EM). ME2 waters show some relationship to ME1. The projection onto C1/C2 and C1/C3 planes reveal that ME3 waters are closely associated with code U3 in plane C1/C2. Only in the plane C2/C3 ME3 and U3 are well separated. Ain Himma is well separated from Hammat Gader and Mukheibeh (U1-U3) in the C1/C2 plane. This way, Fig. 7 visualizes different trends and groupings of waters and brines in the LYG. The different code groups form either clusters or strings in space, thereby indicating constant or variable mixtures, respectively.

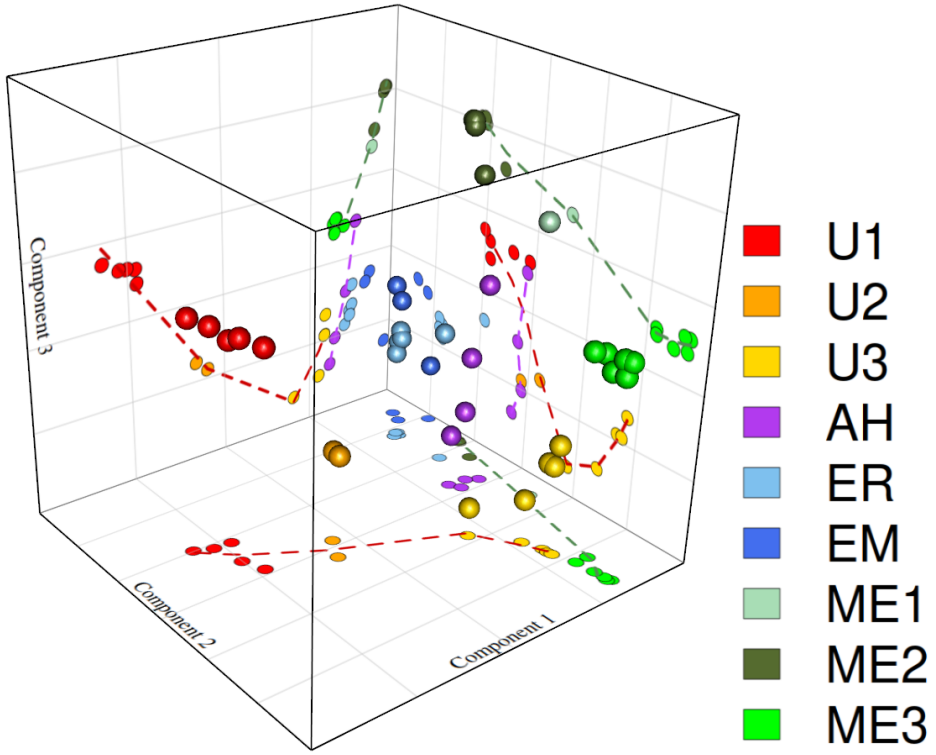

Figure 7. 3D visualization of the clustering of the water samples along the first three principal components. The different colors of large spheres in three-dimensional space and the corresponding colored dots on the projection planes visualize the differences in composition of the groundwater in the Yarmouk Gorge subdivided into nine code groups (Table 1). This plot is based on concentrations in mg/l.

4.2. Mixing of basaltic-rock- and limestone water

The cross plot of ε_{bw} and ε_{lmst} shows the distribution of the various types of water mixtures along the diagonal line (Fig. 8). The red cross marks the arrays of either dominantly limestone- or basaltic rock groundwater. The pure limestone water is presented by Mezar 2 and Mukheibeh 8 in the year 2013; the most basaltic-rock groundwater is among the Mukheibeh ones. Hammat Gader, Ain Himma and Mezar 3 cover the range of ε_{bw} between zero and 0.5. Most of the Mukheibeh waters (U1 and U2) are of the basaltic-water type, whereas the Mukheibeh subgroup U3 (with one exception) and the remaining groundwaters are of limestone water type.

The Mukheibeh field is characterized by mixing of basaltic rock- and Ajloun limestone water with ε_{brine} of 0.0019–0.004 of Ha'On brine (Table 3); in Ain Himma water ε_{brine} varies between 0.0086 and 0.015. When fitting Hammat Gader and the Mezar waters to mixtures of Golan limestone- and basaltic rock water and Ha'On brine, ε_{brine} range between 0.019 and 0.031 for Hammat Gader and ME1 and ME 2. In contrast, ME3 reveals ε_{brine} between 0.0022–0.0039 resembling Mukheibeh water. Substituting the Ha'on brine by Rosh Pinna brine in Hammat Gader and Mezar 1 and 2, the ε_{brine} decline to 0.013–0.028 (Table A2a) as the result of the enhanced chlorinity of Rosh Pinna which is 36 % higher than in Ha'On brine (Table 2). The maximum of volume of brine fraction is 0.03; The cross plots of ε_{bw} and ε_{brine} suggests three different trends (Fig. 9a). The low ε_{brine} values of Mukheibeh water slightly increase with ε_{bw}. Although Ein Sahina and Ain Saraya discharge in the area of Hammat Gader, they plot together with Mezar 3 and the Mukheibeh data. The trend of Hammat Gader and Mezar wells 1 and 2 show the highest ε_{brine} fraction, while Ain Himma plots at slightly lower ε_{brine}.

Preprints (www.preprints.org) | NOT PEER-REVIEWED | Posted: 28 February 2020 doi:10.20944/preprints202002.0414.v1

Peer-reviewed version available at Water 2020, 12, 1291; doi:10.3390/w12051291

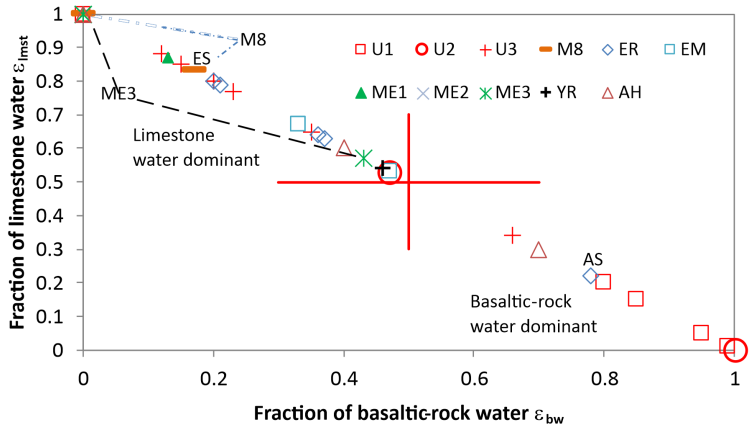

Figure 8. Cross plots of fractions of basaltic-rock- and limestone water in the LYG. Hammat Gader and Mezar are based on Golan limestone water; Muhkeibeh water is related to Ajloun limestone water. M=Mukheibeh sample.

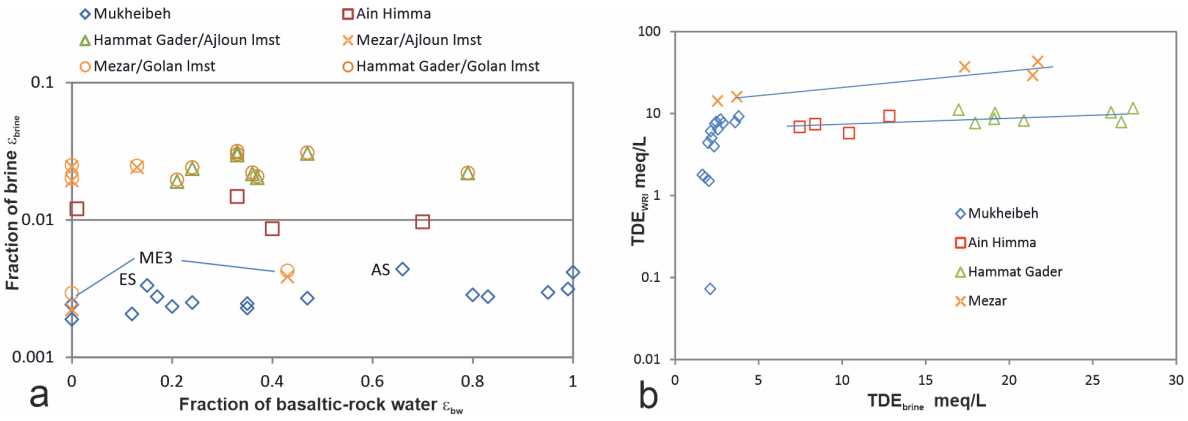

Figure 9. Cross plots of ε_{bw} and ε_{brine} and TDE_{brine} and TDE_{WRI}. These data are obtained under the assumption that ε_{brine} can be estimated after Eq. 2. Hammat Gader and Mezar data are based on Golan limestone water and Ha'On brine. Muhkeibeh water is related to Ajloun limestone water.

4.3. Contributions by water/rock interaction

Following the two suggested approaches of salinization in chapter 3.2, two results are obtained depending on the origin of Cl^- either from brine (Eq. 3) or from halite in evaporites. Both ways of estimations are documented in Table A2 and Table 3 shows the main results. The approach of ε_{brine} by Eq. 3 yields the maximum of TDE_{brine} and the minimum of TDE_{brine} (Table A2), whereas $\varepsilon_{brine} = 0$ yields the maximum of $TDE_{WRI+brine}$ in Table 3. TDE_{WRI} increases over two orders of magnitude in Mukheibeh groundwater. Contrastingly, the increase of TDE_{WRI} in Mezar, Ain Himma and Hammat Gader is less than factor of two (Fig. 9b). The contribution of TDE from water/rock interactions (TDE_{WRI}) is less than by brine (TDE_{brine}) in Hammat Gader and Mezar and most of Ain Himma samples.

From the estimated species *i* of WRI or WRI+brine (Table A2) the amounts of dissolved gypsum and calcite is given by $SO_4^{2-}/2$ and $(Ca^{2+} - SO_4^{2-})/2$ in mmol/l in Table 3. The amount of halite equals the amount of Cl^- in meq/l. (-) signs indicate precipitation; (+) values show dissolution. Calcite shows precipitation when fitting Hammat Gader and Mezar waters with Ajloun limestone water, which is not the case when using Golan limestone water. The composition of brines from Hammat Gader and groundwater from Mezar 1 and 2 is estimated for various combinations of brines and fresh waters. The results of these mixing estimates are compiled in the lower part of Table A2 and Table 3. The differences in mixing either Ajloun or Golan limestone water with either Ha'On or Rosh Pinna brines yield similar

Table 3. Compilation of TDE values, brine fraction ebrine, and mineralogical composition of WRI and WRI+brine.

Code	Location	Sampling date	ΣTDE	TDE_{BW}	TDE_{est}	TDE_{brine}	TDE_{WRI}	ε_{bw}	ε_{brine}	ε_{brine} after Eq.(3) diss(+)/precip(-)		$\varepsilon_{brine} = 0$ after Eq.(6) diss(+)/precip(-)		
Group		year	meq/l							Gypsum	Calcite	Gypsum	Calcite	Halite
										mmol/l		mmol/l		
Estimates based on basalic-rock-, Ajloun limestone water and Ha'On brine														
U-1	Mukheibeh 2	2016	15.07	5.47	6.09	2.57	6.41	0.95	0.00	0.47	0.56	0.47	0.62	1.25
U-1	Mukheibeh 4	2016	15.79	0.00	12.37	1.63	1.79	0.00	0.00	0.48	-0.89	0.49	-0.85	0.79
U-1	Mukheibeh 4	2013	16.75	4.78	6.88	2.39	7.48	0.83	0.00	0.45	0.83	0.46	0.88	1.16
U-1	Mukheibeh 2		16.98	5.70	5.83	2.72	8.43	0.99	0.00	0.48	1.07	0.49	1.13	1.32
U-1	Mukheibeh 1	2001	17.42	4.61	7.08	2.46	7.87	0.80	0.00	0.45	0.66	0.46	0.72	1.20
U-2	Mukheibeh 6	2016	17.23	5.76	5.76	3.60	7.87	1.00	0.00	0.50	0.79	0.51	0.87	1.75
U-2	Mukheibeh 7	2016	15.57	2.71	9.27	2.33	3.98	0.47	0.00	0.26	0.12	0.26	0.17	1.13
U-3	Mukheibeh 10	2016	14.58	1.15	11.05	2.03	1.50	0.20	0.00	0.30	-0.68	0.30	-0.63	0.99
U-3	Mukheibeh 5	2016	15.04	0.69	11.58	1.79	1.66	0.12	0.00	0.27	-0.80	0.27	-0.76	0.87
U-3	Mukheibeh 11	2016	16.43	2.02	10.06	1.97	4.40	0.35	0.00	0.44	-0.46	0.45	-0.42	0.96
U-3	Mukheibeh 9	2016	21.00	3.80	8.01	3.80	9.19	0.66	0.00	0.10	-0.19	0.11	-0.10	1.85
U-3	Mukheibeh 8	2013	14.53	0.00	12.36	2.10	0.07	0.00	0.00	0.18	-0.99	0.18	-0.95	1.02
U-3	Mukheibeh 8	2016	13.33	0.98	11.24	2.39	-0.29	0.17	0.00	0.02	-0.77	0.02	-0.73	1.16
U-3	Mukheibeh 13	2016	14.53	1.38	7.33	2.17	5.02	0.24	0.00	0.24	1.17	0.25	-0.50	1.06
U-3	Mukheibeh 13	2013	15.32	2.02	7.11	2.13	6.08	0.35	0.00	0.18	1.39	0.15	0.01	1.04
U-3	Ein Sahina	2016	16.48	0.86	5.93	2.88	7.66	0.15	0.00	0.44	1.38	0.40	-0.44	1.15
AH	Ain Himma	2007	32.32	1.90	10.19	12.83	9.30	0.33	0.01	2.07	-1.48	2.10	-1.18	6.24
AH	Ain Himma	2001	28.47	0.06	12.31	10.41	5.75	0.01	0.01	1.41	-1.44	1.44	-1.19	5.06
AH	Ain Himma	2013	24.04	2.30	9.73	7.45	6.85	0.40	0.01	1.18	-0.20	1.19	-0.03	3.62
AH	Ain Himma	2016	23.53	4.03	7.74	8.39	7.40	0.70	0.01	1.21	0.04	1.23	0.24	4.08
Estimates based on basalic-rock-, Golan limestone water and Ha'On brine														
AS	Ain Saraya	2016	33.51	4.55	5.78	19.11	8.63	0.79	0.02	1.11	1.00	1.15	1.45	9.29
EB	Ein Balsam	2016	31.43	2.13	5.82	17.96	7.65	0.37	0.02	1.27	0.86	1.31	1.28	8.73
ER	Ein Reach	2016	34.91	1.38	5.83	20.87	8.21	0.24	0.02	1.22	1.16	1.27	1.65	10.15
ER	Ein Reach	2000	33.95	1.21	5.83	16.97	11.15	0.21	0.02	1.09	1.71	1.13	2.11	8.25
ER	Ein Reach	2004	35.11	2.07	5.82	19.15	10.14	0.36	0.02	1.12	1.34	1.17	1.79	9.31
EM	Ein Makla	2016	40.38	2.71	5.81	26.70	7.87	0.47	0.03	1.42	1.17	1.48	1.80	12.98
EM	Ein Makla	2000	44.88	1.90	5.82	27.41	11.65	0.33	0.03	1.51	1.85	1.58	2.50	13.33
EM	Ein Makla	2004	42.23	1.90	5.82	26.10	10.32	0.33	0.03	1.44	1.29	1.50	1.91	12.69
ME1	Mezar 1	2016	29.05	0.75	5.84	21.41	1.80	0.13	0.02	0.02	0.45	0.07	0.96	10.41
ME2	Mezar 2	2016	43.01	0.00	5.85	21.71	15.45	0.00	0.02	3.42	0.07	3.47	0.59	10.56
ME2	Mezar 2	2001	37.01	0.00	5.85	17.34	13.82	0.00	0.02	2.80	0.11	2.85	0.52	8.43
ME3	Mezar 3	2016	16.05	2.48	5.81	3.70	6.54	0.43	0.00	0.12	1.12	0.09	-0.05	1.63
ME3	Mezar 3	2001	14.20	0.00	5.85	2.54	5.81	0.00	0.00	-0.01	1.39	-0.07	-0.77	0.94
Estimates based on basalic-rock-, Golan limestone water and Rosh Pinna brine														
AS	Ain Saraya	2016	33.51	4.55	5.78	19.21	8.52	0.79	0.01	0.98	-0.11	1.15	1.45	9.29
EB	Ein Balsam	2016	31.43	2.13	5.82	18.06	7.55	0.37	0.01	1.15	-0.18	1.31	1.28	8.73
ER	Ein Reach	2016	34.91	1.38	5.83	20.99	8.09	0.24	0.02	1.08	-0.05	1.27	1.65	10.15
ER	Ein Reach	2000	33.95	1.21	5.83	17.06	11.06	0.21	0.01	0.98	0.73	1.13	2.11	8.25
ER	Ein Reach	2004	35.11	2.07	5.82	19.25	10.04	0.36	0.01	1.00	0.23	1.17	1.79	9.31
EM	Ein Makla	2016	40.38	2.71	5.81	26.85	7.72	0.47	0.02	1.24	-0.37	1.48	1.80	12.98
EM	Ein Makla	2000	44.88	1.90	5.82	27.57	11.50	0.33	0.02	1.33	0.26	1.58	2.50	13.33
EM	Ein Makla	2004	42.23	1.90	5.82	26.24	10.17	0.33	0.02	1.26	-0.22	1.50	1.91	12.69
ME1	Mezar 1	2016	29.05	0.75	5.84	21.53	1.68	0.13	0.02	-0.12	-0.79	0.07	0.96	10.41
ME2	Mezar 2	2016	43.01	0.00	5.85	21.83	15.33	0.00	0.02	3.27	-1.18	3.47	0.59	10.56
ME2	Mezar 2	2001	37.01	0.00	5.85	17.43	13.73	0.00	0.02	2.69	-0.90	2.85	0.52	8.43
ME3	Mezar 3	2016	16.05	2.48	5.81	3.72	6.52	0.43	0.00	0.09	0.91	0.13	1.21	1.80
ME3	Mezar 3	2001	14.20	0.00	5.85	2.56	5.80	0.00	0.00	-0.03	1.24	-0.01	1.45	1.24

results for gypsum dissolution but significantly different ones for solution of calcite. In the presence of brines, calcite is precipitated from Ajloun limestone water, whereas in Golan limestone calcite dissolves. In absence of brine, some Hammat Gader waters dissolve calcite and Mezar groundwater precipitate calcite when fitted to Golan limestone water. The estimates reveal dissolution of significant amounts of gypsum and calcite in waters from Ain Himma, springs of Hammat Gader and well Mezar 2, whereas Mukheibeh waters dissolve much smaller amounts of both minerals (Table 3). The dissolution of calcite and gypsum leads to enhancement of Ca^{2+} in Mukheibeh groundwater (Fig. 5e). The increase of Mg^{2+} in groundwater (Fig. 5f) is caused by high Mg^{2+} concentration in the admixed Ha'On brine.

The cross plots of calcite and gypsum reveal that their amounts are very similar and independent on the absence or presence of brine Eq. 2. Gypsum is always dissolved but calcite is both dissolved in Hammat Gader, Mezar and part of the Muhheibeh waters and precipitated in the other part of Mukheibeh and Himma water (Fig. 10).

The cross plots of halite and gypsum dissolution only reveal two trends between Mukheibeh at one end and either Hammat Gader waters or Mezar and Himma waters at the other end (Fig. 11).

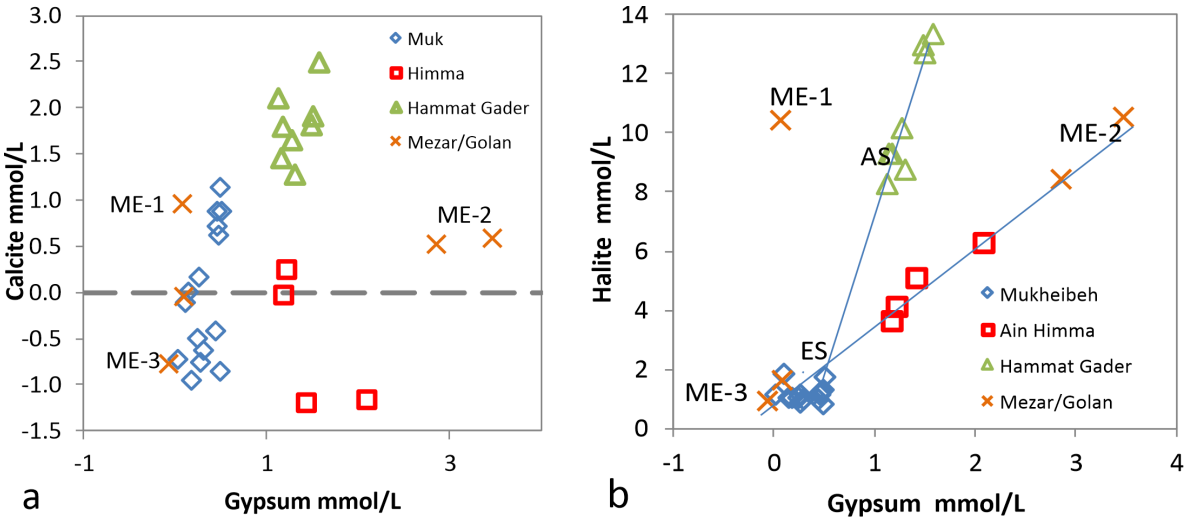

Figure 10. Cross plots of minerals. (a) Amounts of gypsum and calcite in WRI based on the assumption that ε_{brine} can be estimated after Eq. 2. (b) Amounts of halite and gypsum in WRI+brine. Here ε_{brine} is assumed to be zero and its contribution appear together with those of the WRI.

5. Discussion

5.1. Saline contributions to groundwater

Although the process of estimating the contributions of basaltic-rock- and limestone water may not be as precise as the figures suggest, the volume contribution of brine is always less than 3 volume-%. Because the fractions of basaltic-rock- and limestone water are based on interpretations of REY patterns, it should be kept in mind that the limestone water may have already dissolved some gypsum and halite. This may lead to too high brine- and limestone water fractions due to which the fraction of basaltic-rock water is lowered. For similar reasons the true contribution of WRI may be slightly higher than derived in Table 3. Possible atmospheric contributions are minimized by selecting basaltic-rock- and limestone water with lowest Cl^- concentrations.

The triplot visualizes the differences of the various local groundwater and brines (Fig. 11). The contributions $TDE_{WRI+brine}$, TDE_{bw} and TDE_{lmst} in groundwaters show a narrow cluster of Mezar wells 1 and 2, Hammat Gader and Ain Saraya samples, whereas water from Mukheibeh well field, Ain Himma and Mezar 3 cover a wide field between the dashed lines. The contributions in TDE from brine and WRI ranges between 10 and 70 %, 80-90 % in Mukheibeh, Ain Himma and Mezar 3 and

in Hammat Gader and Mezar wells 1 and 2, respectively. These estimates do not really differ, if the sources of limestones water or brines are varied.

The Mukheibeh groundwater originates from an aquifer with constant contribution of brine but increasing dissolution of gypsum (Fig. 9b). Calcite in code group U3 and Ain Himma is always precipitated (Table 3) contrasting the mixing in Hammat Gader, and Mezar wells 1 and 2. The mixture of Mt. Hermon/Golan limestone water and Ha'On brine in Mezar 2 distinctly differs from Hammat Gader by enhanced contributions by WRI (Figs. 7, 9 and 11).

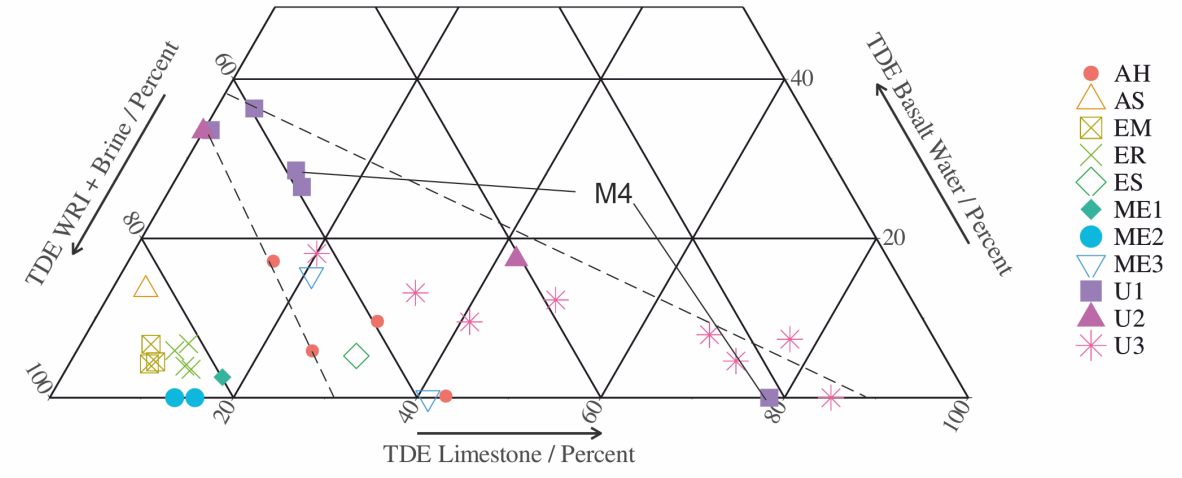

Figure 11. Ternary plot of contributions in %-TDE of basaltic-rock-water, limestone water and WRI+brine. Several trends evolve. All trends seem to culminate in the Yarmouk River water. The dashed lines fix the array of Mukheibeh, Ain Himma, Mezar 3 and Ein Sahina. Clearly separated, the waters from Hammat Gader (EM, ER), Mezar 1 and 2, and Ain Saraya cluster in the lower left corner.

In assumed absence of brine the dissolution of halite amounts to about 1 mmol/l for Mukheibeh and Mezar 3, about 4-6 mmol/l in Ain Himma, and between 8 and 13 mmol/l in Hammat Gader and Mezar wells 1 and 2 (Table 3; Fig. 11). Independent on the type of estimates, the dissolution of gypsum varies between 0 and 0.5 mol/l in Mukheibeh and Mezar wells 1 and 3 waters. It ranges from 1–3.5 mmol/l in Ain Himma, Hammat Gader and Mezar 2.

In absence of deep brines, gypsum and calcite are dissolved in Hammat Gader and Mezar 1 and 3 in Golan limestone water. In the presence of Rosh Pinna brine instead of Ha'On brine, calcite often has to be precipitated making the former less reasonable because the limestone water is already saturated with respect to calcite. Mezar 3 does not dissolve gypsum but calcite particularly in the presence of Rosh Pinna brine (Table 3). Taking Ajloun limestone water and Ha'On brine calcite is precipitated from groundwater of Hammat Gader and Mezar (Table A2) suggesting that Ajloun water does not play any in these waters.

All groundwater mixes with brine being present in aquifer rocks and interact with aquifer rocks. The contribution of brine dominates the salinity of groundwater. The Tortonian Ha'On brine is identified in the study area. It is reasonable to assume that this brine infiltrated the Cretaceous (and probably Jurassic) limestone aquifers and is therefore omnipresent in the surroundings of the Yarmouk Gorge [43]. Estimates based on the contributions of Rosh Pinna brine abundantly lead to dissolution of calcite when applying Eq. 2 which is unreasonable because in limestone aquifers calcite saturation should be attained.

5.2. Groundwater divide between the Ajloun and the Golan Heights

Chemical similarities suggest that Mezar 3 on the northern Yarmouk River bank but located very near to the LYF produce groundwater of the Mukheibeh type (Fig. 3). Ein Sahina and M5, both north of LYF, produce water of the Mukheibeh type (Table 1). Ain Saraya south of the Yarmouk River just

opposite of Hammat Gader but north of LYF produces water typical for Hammat Gader (Table 1). Ain Himma located southwest of the Yarmouk River but north of the LYF is seemingly related to Hammat Gader brines (Fig. 5). The thermohaline water of Hammat Gader seems to ascend along faults from greater depth. These examples of distribution of salinized groundwater indicate that probably not the Yarmouk River but the LYF delineates the groundwater divide between the Ajloun and the Golan Heights. LYF clearly separates the Mukeibeh well field with $0.002 < \varepsilon_{\text{brine}} < 0.004$ from the Mezar well field ($0.02 < \varepsilon_{\text{brine}} < 0.04$), Ain Himma ($0.009 < \varepsilon_{\text{brine}} < 0.013$) and Hammat Gader region ($0.02 < \varepsilon_{\text{brine}} < 0.04$).

Although the LYF follows the trend of the Yarmouk River the chemical composition of local groundwater and brines is oriented according to the LYF and not to the political border between Jordan and Israel given by the Yarmouk River. According to the regional differences the transboundary flow may be influenced by local pumping on the Israeli side, the artesian outflow on the Jordanian side, and recharge of the common aquifer on both sides of the LYF.

In well and spring water of the Mezar field and Hammat Gader region significant changes in REY patterns [52] indicate variation in groundwater flow and mixing of basaltic-rock- and limestone waters (Fig. 4b). Mezar 3 in 2008 produced water with the same REY pattern of Mezar 2 which definitely originates from the deep aquifer in the Golan. In Fig. 11 Mukheibeh 2, 4 and 8 show high variations in composition within the Mukheibeh array of dashed lines. This behavior suggests that their flow system probably depends on pumping and recharge. The most extremely different compositions reveal waters from the wells Mezar 2 (depth -807 m) and Mezar 3 (depth -102 m), drilled few tens of meters apart. Mezar 3 water in 2001 and 2016 was of the Mukheibeh type (Fig. 2). In 2008, Mezar 2 and 3 showed the same type of REY patterns which do not fit into Fig. 4a [52].

Figs. 5, 6, 7, 9 and 11 suggest different aquifers. The uppermost fresh water aquifer producing the Mukheibeh type is dominantly recharged by either basaltic-rock- or limestone water. Part of the infiltrated water penetrate into deeper aquifers and leach along their flow paths evaporites and relics of brine. The deepest aquifer is that of Mezar 2. Hammat Gader originates from an aquifer which enables much less contact with gypsum but slightly more with halite, whereas Mezar 2 and Himma water had more contact with gypsum and less halite.

6. Conclusion

The basaltic-rock groundwaters from the Hauran Plateau mix with limestone water from either the Ajloun or the Golan Heights depending on the position of springs and wells south or north of the Lower Yarmouk fault respectively. The most basaltic-rock-dominated waters occur in the center of the Mukheibeh well field defined by wells 1, 2 and 4. The limestone-dominated waters are mainly present in the region of Mezar and Hammat Gader. Running sub-parallel to the Yarmouk River, the LYF seems to be the actual groundwater divide between the Ajloun and the Golan Heights.

Ein Sahina and Mukheihbeh 5, north and southwest of of Hammat Gader, respectively, and Mezar 3 resemble in composition the Mukeihbeh water (Table 1) but are located north of the LYF. The variability of Ain Himma composition sometimes resembles that of Mezar 2 suggesting groundwater from great depth. Ain Saraya south of the Yarmouk River and opposite of Hammat Gader produces the same type of saline water from north of the LYF. Since the Yarmouk River represents the international border between Jordan and Israel, these examples suggest only in a political sense some transboundary flow over short distances possibly through local N-S trending faults and fissures beneath the river but do not impugn the general barrier character of the LYF in respect to regional groundwater flow crossing beneath the Gorge.

The salinity of groundwater is mainly due to (i) leaching of remnants of Tertiary Rift brine but not of mixtures of relicts of the Triassic brine with the former and (ii) water/rock interaction such as dissolution of gypsum and calcite. The basaltic-rock-dominated waters show the lowest salinities, whereas the waters of Hammat Gader and Mezar 2 manifest the highest salinity. Only the basaltic-rock

waters show higher TDE_{WRI} than TDE_{brine}. The contribution of atmospheric precipitation is considered part of the recharge water or to be negligible in water with lowest Cl^- concentrations.

The uniform trend of Mg^{2+} with Cl^- in all groundwater excepting the Mukeheibeh ones suggest leaching of the Tertiary Ha'On brine which is of Mg^{2+}-Cl^- type. The different dilution trends of other dissolved species such as Na^+, K^+, Ca^{2+} Br^- and SO_4^{2-} of either Hammat Gader or Mezar/Ain Himma indicate differences in occurrences of evaporite minerals in the respective aquifers.

Author Contributions: CreDiT taxonomy: Conceptualization: PM; Methodology: PM, MDL, CS; Data Curation: CS; Writing, original draft: PM; Writing, Review & Editing: CS, MDL, NI, FM, ER, ES; Visualization: PM, MDL, NI; Supervision: PM; Project Administration & Funding Aqusition: FM.

Funding: Authors gratefully acknowledge the DFG funding support (grant Ma4450/2) in the frame of a trilateral program to support peaceful development in Middle East.

Acknowledgments: We thank various members of the local water authorities enabling sampling along the Yarmouk River. The assistance of Dr. M. Raggad during sampling is gratefully acknowledged.

Conflicts of Interest: The authors declare not to have any conflict of interest.

Abbreviations

The following abbreviations are used in this manuscript:

LYG	Lower Yarmouk Gorge
WRI	Water/rock interaction
LYF	Lower Yarmouk fault
ε_{brine}	Volume-fraction of brine
ε_{bw}	Volume-fraction of basaltic-rock water
ε_{lmst}	Volume-fraction of limestone water
$c_{i,bw}$	Concentration of species *i* in basaltic-rock water
$c_{i,brine}$	Concentration of species *i* in brine
$c_{i,agw}$	Concentration of species *i* in analyzed groundwater
$c_{i,WRI}$	Concentration of species *i* due to WRI
TDE_{bw}	Total dissolved equivalents due to weathered basalt
TDE_{lmst}	Total dissolved equivalents due to dissolved limestones
TDE_{agw}	Total dissolved equivalents in analyzed groundwater
TDE_{brine}	Total dissolved equivalents in brine
TDE_{est}	Total dissolved equivalents of estimated mixture of basaltic-rock- and limestone water
TDE_{WRI}	Total dissolved equivalents due to water/rock interaction
$TDE_{WRI+brine}$	Total dissolved equivalents due to water/rock interaction and mixing with brine

Table A1. Analyses of Ha'On brine, Triassic brines of Rosh Pinna, basaltic spring waters from the Golan Heights and the Hauran Plateau and limestone waters from the Ajloun Mts and Golan Heights. Because the analyses of Ha'On brine are from different wells for each group the average and % standard deviation is given. The extrapolated concentrations of Mg^{2+}, K^+, Na^+, Cl^- and Br^- of the original Ha'On are derived from data on evaporated seawater [23,37]

Reference	Well	Sampling date	Ca^{2+} mg/l	Mg^{2+} mg/l	K^+ mg/l	Na^+ mg/l	Cl^- mg/l	SO_4^{2-} mg/l	Br^- mg/l	HCO_3^- mg/l	Na/Cl eq.ratio	1000Br/Cl eq.ratio	Mg/Ca eq.ratio
Extrapolated original Ha'On (Fig. 6)				47500	14200	50000	184000		2250		0.42	5.43	
Late Tertiary Ha'On brine													
Mandel 1965	D-1071	1961	1476	2100	317	8633	21971	32.5	266.6	384	0.61	5.38	2.34
Mandel 1965	D-1071	1964	1427	2141	285	8990	22624	tr	153.2	341	0.61	3.00	2.47
Mandel 1965	D-1071	1965	1285	2258	296	9093	23045	3.7		186	0.61		2.89
	Average		1396	2166	299	8906	22547	18	210	304	0.61	4.13	2.55
	Dilution factor			*22*	*47*	*6*	*8*		*11*				
Bergelson et al. 1999	D-1071	1993	593	971	409	4040	9600	112	109	427	0.65	5.04	2.69
Bergelson et al. 1999	D-1071	1993	589	1000	414	4209	10188	98.6		537	0.64		2.79
	Average		591	985	411	4125	9894	106	109	482	0.64	4.89	2.74
	Dilution factor			*48*	*35*	*12*	*19*		*21*				
Mandel 1965	D-1072	1961	653	1645	185	6103	14670	117	179	1195	0.64	5.41	4.15
Bergelson et al. 1999	D-1072	1993	599	1140	262	4382	11394	27.4	131	439	0.59	5.10	3.13
Bergelson et al.1999	D-1072	2000	1078	1657	442	5212	15800	59.8	207	504	0.51	5.81	2.53
Siebert et al. 2014	D-1072	2004	758	1169	394	4276	11668	644	133	576	0.56	5.07	2.54
	Average		772	1403	321	4993	13383	212	163	678			
	Dilution factor			*34*	*44*	*10*	*14*		*14*				
Klein BenDavid et al. 2014	D-1072	2003	559	910	425	3687	8486	765	95.6	548	0.67	5.00	2.68
	Dilution factor			*52.2*	*33.4*	*13.6*	*21.7*		*23.5*				
	Ha'On average		**902**	**1499**	**343**	**5863**	**14945**	**207**	**159**	**514**	**0.60**	**4.73**	**2.74**
	Dilution factor			*31.7*	*41.4*	*8.5*	*12.3*		*14.1*				
Triassic brine		depth											
Starinski 1974	Rosh Pinna 1	3845-3864	26946	2918	1157	33415	105349	347		171	0.49		0.18
Starinski 1974	Rosh Pinna 1	2486-2586	4794	724	358	8004	22819	1161		370	0.54		0.25
Limestone water from Mt. Hermon Massif													
Sie 786/08	Ein Dan	2008	65.9	5.4	0.7	4.3	9.8	9.0			0.68		0.14
Sie 787/08	Ein Banyas	2008	72.3	12.4	1.5	9.9	12.9	57.3			1.18		0.28
	Average		69.1	8.9	1.1	7.1	11.3	33.1			0.97		0.21
Limestone water from the Ajloun													
Siebert et al. 2014	Ain Al Azal		96.0	16.8	0.6	16.1	32.4	14.6		291			
Siebert et al. 2014	Ain Al Murarar		101	8.04	2.29	16.6	24.3	6.06		277			
	Average		98.6	12.4	1.43	16.4	28.3	10.337		284			
Limestone water from the Golan													
Siebert et al. 2014	Alonei HaBashan 3		9.9	8	4.6	43.3	17.2	4.9		132			
Siebert et al. 2014	Allonei HaBashan 8		5.63	3.97	3.31	56.2	18.4	4.695		124			
	Average		7.77	5.99	3.96	49.8	17.8	4.7975		128			
Basaltic-rock water from Golan Heights and Hauran Plateau													
Dafny et al. 2006	Average (n=60)		30.8	17.2	3.8	27.8	29.7	10.8	0.022	177	1.44	0.33	0.92
Kattan 1997	Average (n=21)		26.8	12.1	3.6	25.9	29.6	15		126			
	Weighted average		29.8	15.9	3.75	27.3	29.7	11.9	0.022	164			

Table A2. Estimation of brine and water/rock contribution to salinity of groundwaters. (a) The contribution of the basaltic-rock water, the sum of basaltic rock- and limestone water, the contribution of brine are estimated based on brine after Eq. 2. The difference of analyzed and estimated concentrations yield the contribution of water/rock interaction here presented as gypsum and calcite dissolution. (b) Similar to (a) but brine is set to zero. Consequently only the sum of water/rock interaction and brine is obtained.

			Estimated groundwater $c_{gw}=c_{fw}+c_{rock}$								Contribution of brine to estimated groundwater c_{gw}								$\varepsilon_{brine}=0$										$\varepsilon_{brine}>0$									
																			Difference of meas. & estd. conc.: $c_{rock}=c_{gw}-c_{brine}$										Difference of meas. & estd. conc.: $c_{wb}=c_{gw}-c_{brine}$									
Code	Source	Year	Ca	Mg	K	Na	Cl	SO4	HCO3	TDE_{gw}	Ca	Mg	K	Na	Cl	SO4	HCO3	TDE_{brine}	Ca	Mg	K	Na	SO4	HCO3	TDE_{WR}	Gypsum	Calcite	Ca	Mg	K	Na	Cl	SO4	HCO3	TDE_{WB}	Gypsum	Calcite	Halite
			meq/l								meq/l								meq/l							mmol/l		meq/l								mmol/l		
Estimates based on basaltic-rock-, Ajloun limestone water and Ha'On brine																																					
U-1	Mukheibeh 2	2016	1.702	0.577	0.818	0.074	0.343	0.219	2.358	6.091	0.13	0.37	0.03	0.76	1.25	0.01	0.02	2.57	2.06	1.20	-0.77	0.87	0.94	2.12	6.41	0.47	0.56	2.20	1.56	-0.74	1.62	1.25	0.95	2.14	8.98	0.47	0.62	1.25
U-1	Mukheibeh 4	2016	4.929	1.024	0.037	0.712	0.799	0.215	4.657	12.373	0.09	0.23	0.02	0.48	0.79	0.01	0.02	1.63	-0.81	1.05	0.02	0.55	0.97	0.02	1.79	0.48	-0.89	-0.73	1.28	0.04	1.03	0.80	0.97	0.04	3.42	0.49	-0.85	0.79
U-1	Mukheibeh 4	2013	2.109	0.634	0.719	0.155	0.401	0.219	2.648	6.885	0.12	0.34	0.02	0.70	1.16	0.01	0.02	2.39	2.57	1.41	-0.67	0.82	0.91	2.44	7.48	0.45	0.83	2.69	1.75	-0.64	1.52	1.16	0.92	2.46	9.87	0.46	0.88	1.16
U-1	Mukheibeh 2	2013	1.566	0.558	0.851	0.047	0.324	0.220	2.261	5.827	0.14	0.39	0.03	0.80	1.32	0.01	0.03	2.72	3.09	1.52	-0.80	0.83	0.96	2.82	8.43	0.48	1.07	3.23	1.91	-0.77	1.64	1.32	0.97	2.85	11.15	0.49	1.13	1.32
U1	Mukheibeh 1	2001	2.211	0.648	0.695	0.175	0.415	0.219	2.721	7.083	0.13	0.35	0.03	0.73	1.20	0.01	0.02	2.46	2.23	1.47	-0.64	0.80	0.90	3.12	7.87	0.45	0.66	2.35	1.82	-0.62	1.52	1.20	0.91	3.14	10.33	0.46	0.72	1.20
U-2	Mukheibeh 6	2016	1.532	0.554	0.859	0.041	0.319	0.220	2.237	5.761	0.19	0.51	0.04	1.06	1.75	0.02	0.03	3.60	2.58	1.32	-0.81	1.03	1.01	2.74	7.87	0.50	0.79	2.77	1.83	-0.77	2.09	1.75	1.03	2.77	11.47	0.51	0.87	1.75
U-2	Mukheibeh 7	2016	3.332	0.803	0.423	0.396	0.574	0.217	3.520	9.265	0.12	0.33	0.02	0.69	1.13	0.01	0.02	2.33	0.75	1.25	-0.37	0.66	0.51	1.19	3.98	0.26	0.12	0.87	1.58	-0.35	1.34	1.13	0.52	1.21	6.31	0.26	0.17	1.13
U-3	Mukheibeh 10	2016	4.250	0.930	0.201	0.578	0.703	0.216	4.173	11.051	0.11	0.29	0.02	0.60	0.99	0.01	0.02	2.03	-0.76	0.84	-0.13	0.87	0.60	0.08	1.50	0.30	-0.68	-0.65	1.13	-0.11	1.47	0.99	0.61	0.10	3.53	0.30	-0.63	0.99
U-3	Mukheibeh 5	2016	4.522	0.967	0.136	0.631	0.741	0.216	4.367	11.579	0.09	0.26	0.02	0.53	0.87	0.01	0.02	1.79	-1.06	0.75	-0.06	0.88	0.53	0.62	1.66	0.27	-0.80	-0.97	1.01	-0.04	1.41	0.87	0.54	0.63	3.46	0.27	-0.76	0.87
U-3	Mukheibeh 11	2016	3.740	0.859	0.325	0.477	0.631	0.217	3.810	10.059	0.10	0.28	0.02	0.58	0.96	0.01	0.02	1.97	-0.04	2.07	-0.27	0.85	0.88	0.90	4.40	0.44	-0.46	0.06	2.35	-0.25	1.44	0.96	0.89	0.92	6.37	0.45	-0.42	0.96
U-3	Mukheibeh 9	2016	2.687	0.713	0.579	0.269	0.482	0.218	3.060	8.009	0.20	0.54	0.04	1.12	1.85	0.02	0.04	3.80	-0.18	1.13	-0.21	3.83	0.20	4.43	9.19	0.10	-0.19	0.01	1.67	-0.17	4.95	1.85	0.22	4.46	12.99	0.11	-0.10	1.85
ME3	Mukheibeh 8	2013	4.917	1.024	0.037	0.712	0.799	0.215	4.657	12.361	0.11	0.30	0.02	0.62	1.02	0.01	0.02	2.10	-1.63	0.32	0.08	0.99	0.35	-0.04	0.07	0.18	-0.99	-1.53	0.62	0.10	1.61	1.02	0.36	-0.02	2.16	0.18	-0.95	1.02
U-3	Mukheibeh 8	2016	4.338	0.944	0.177	0.598	0.717	0.216	4.246	11.235	0.12	0.34	0.02	0.70	1.16	0.01	0.02	2.39	-1.51	0.36	-0.07	1.13	0.04	-0.24	-0.29	0.02	-0.77	-1.40	0.70	-0.05	1.84	1.16	0.05	-0.22	2.09	0.02	-0.73	1.16
U-3	Mukheibeh 13	2016	0.663	0.911	0.234	0.551	0.684	0.216	4.076	7.335	0.11	0.31	0.02	0.64	1.06	0.01	0.02	2.17	2.82	0.84	-0.16	0.81	0.48	0.23	5.02	0.24	1.17	-0.51	1.15	-0.14	1.45	1.06	0.49	0.25	3.75	0.25	-0.50	1.06
U-3	Mukheibeh 13	2013	0.788	0.514	0.366	1.421	0.438	0.142	2.148	5.818	0.13	0.36	0.03	0.74	1.23	0.01	0.02	2.53	3.13	1.18	-0.30	-0.27	0.36	2.87	6.97	0.18	1.39	0.31	1.20	-0.23	1.42	1.04	0.29	1.23	5.26	0.15	0.01	1.04
ES	Ein Sahina	2016	0.560	0.502	0.215	1.845	0.475	0.118	2.121	5.836	0.15	0.41	0.03	0.85	1.40	0.01	0.03	2.88	3.64	1.39	-0.16	-0.78	0.89	2.78	7.76	0.44	1.38	-0.07	1.35	-0.08	1.30	1.15	0.80	0.64	5.10	0.40	-0.44	1.15
AH	Ein Himma	2007	3.808	0.869	0.308	0.490	0.641	0.217	3.858	10.191	0.67	1.83	0.13	3.78	6.24	0.06	0.12	12.83	1.19	0.11	-0.08	1.05	4.15	2.89	9.30	2.07	-1.48	1.86	1.94	0.05	4.82	6.24	4.21	3.02	22.13	2.10	-1.18	6.24
AH	Ein Himma	2001	4.895	1.019	0.045	0.705	0.794	0.215	4.633	12.307	0.54	1.48	0.11	3.07	5.06	0.05	0.10	10.41	-0.06	0.37	0.21	1.63	2.82	0.78	5.75	1.41	-1.44	0.48	1.85	0.31	4.69	5.06	2.87	0.88	16.16	1.44	-1.19	5.06
AH	Ein Himma	2013	3.570	0.836	0.366	0.443	0.607	0.217	3.689	9.728	0.39	1.06	0.08	2.19	3.62	0.04	0.07	7.45	1.94	0.74	-0.21	1.03	2.35	1.01	6.85	1.18	-0.20	2.33	1.80	-0.14	3.23	3.62	2.39	1.08	14.31	1.19	-0.03	3.62
AH	Ein Himma	2016	2.551	0.695	0.612	0.242	0.463	0.218	2.963	7.744	0.44	1.20	0.09	2.47	4.08	0.04	0.08	8.39	2.51	0.58	-0.45	1.38	2.43	0.96	7.40	1.21	0.04	2.95	1.77	-0.37	3.84	4.08	2.47	1.04	15.79	1.23	0.24	4.08
AS	Ain Saraya	2016	2.245	0.652	0.686	0.182	0.420	0.219	2.745	7.149	0.99	2.70	0.19	5.59	9.23	0.09	0.18	18.98	3.27	-0.23	-0.57	1.19	2.19	1.54	7.38	1.09	0.54	4.25	2.48	-0.38	6.77	9.23	2.28	1.73	26.36	1.14	0.99	9.23
ER	Ein Balsam	2016	3.672	0.850	0.341	0.464	0.622	0.217	3.762	9.926	0.92	2.50	0.18	5.17	8.55	0.09	0.17	17.58	1.41	-0.56	-0.21	0.01	2.47	0.80	3.93	1.23	-0.53	2.33	1.95	-0.03	5.19	8.55	2.55	0.97	21.51	1.28	-0.11	8.55
ER	Ein Reach	2016	4.114	0.911	0.234	0.551	0.684	0.216	4.076	10.786	1.06	2.91	0.21	6.01	9.92	0.10	0.20	20.41	1.32	-0.77	-0.08	0.40	2.35	0.50	3.71	1.17	-0.51	2.39	2.13	0.12	6.41	9.92	2.45	0.70	24.12	1.23	-0.03	9.92
ER	Ein Reach	2000	4.216	0.925	0.210	0.571	0.698	0.216	4.149	10.984	0.86	2.35	0.17	4.85	8.02	0.08	0.16	16.49	2.04	-0.02	-0.06	0.81	2.10	1.62	6.48	1.05	-0.03	2.90	2.33	0.10	5.66	8.02	2.18	1.78	22.97	1.09	0.36	8.02
ER	Ein Reach	2004	3.706	0.854	0.333	0.470	0.626	0.217	3.786	9.993	0.98	2.67	0.19	5.52	9.12	0.09	0.18	18.76	2.04	-0.28	-0.20	0.80	2.17	1.82	6.36	1.09	-0.07	3.01	2.40	-0.01	6.32	9.12	2.27	2.01	25.12	1.13	0.37	9.12
EM	Ein Makla	2016	3.332	0.803	0.423	0.396	0.574	0.217	3.520	9.265	1.37	3.76	0.27	7.77	12.83	0.13	0.26	26.38	2.79	-1.35	-0.26	0.97	2.78	-0.20	4.73	1.39	0.01	4.17	2.41	0.01	8.73	12.83	2.91	0.06	31.11	1.45	0.63	12.83
EM	Ein Makla	2000	3.808	0.869	0.308	0.490	0.641	0.217	3.858	10.191	1.41	3.85	0.27	7.95	13.13	0.13	0.26	27.00	3.70	-1.08	-0.12	0.79	2.95	1.45	7.69	1.47	0.38	5.11	2.77	0.15	8.74	13.13	3.08	1.72	34.69	1.54	1.01	13.13
EM	Ein Makla	2004	3.808	0.869	0.308	0.490	0.641	0.217	3.858	10.191	1.34	3.66	0.26	7.56	12.49	0.13	0.25	25.69	2.44	-1.07	-0.13	1.07	2.80	1.25	6.35	1.40	-0.18	3.78	2.59	0.13	8.63	12.49	2.93	1.49	32.04	1.46	0.43	12.49
ME1	Meizar 1	2016	4.488	0.963	0.144	0.625	0.737	0.216	4.342	11.513	1.09	2.98	0.21	6.15	10.15	0.10	0.20	20.88	-2.98	-2.54	-0.02	3.23	-0.05	-0.98	-3.34	-0.03	-1.46	-1.89	0.44	0.19	9.38	10.15	0.05	-0.78	17.54	0.02	-0.97	10.15
ME2	Meizar 2	2016	4.929	1.024	0.037	0.712	0.799	0.215	4.657	12.373	1.10	3.01	0.21	6.21	10.26	0.11	0.21	21.10	2.47	-0.98	0.36	2.21	6.72	-1.24	9.53	3.36	-2.12	3.57	2.02	0.58	8.42	10.26	6.83	-1.04	30.64	3.41	-1.63	10.26
ME2	Meizar 2	2001	4.929	1.024	0.037	0.712	0.799	0.215	4.657	12.373	0.87	2.38	0.17	4.92	8.13	0.08	0.16	16.73	1.32	-0.54	0.35	2.11	5.50	-0.82	7.91	2.75	-2.09	2.19	1.84	0.52	7.03	8.13	5.58	-0.66	24.64	2.79	-1.70	8.13
ME3	Meizar 3	2016	3.468	0.822	0.390	0.423	0.593	0.217	3.616	9.530	0.17	0.48	0.03	0.99	1.63	0.02	0.03	3.35	-0.09	0.76	-0.32	0.90	0.17	1.76	3.17	0.08	-0.13	0.08	1.24	-0.29	1.88	1.63	0.19	1.80	6.52	0.09	-0.05	1.63
ME3	Meizar 3	2001	4.929	1.024	0.037	0.712	0.799	0.215	4.657	12.373	0.10	0.28	0.02	0.57	0.94	0.01	0.02	1.93	-1.76	0.42	0.06	0.83	-0.14	0.49	-0.10	-0.07	-0.81	-1.66	0.70	0.08	1.40	0.94	-0.13	0.51	1.83	-0.07	-0.77	0.94
Estimates based on basaltic-rock-, Golan limestone water and Ha'on brine																																					
AS	Ain Saraya	2016	1.292	0.541	0.700	0.486	0.358	0.195	2.208	5.779	1.00	2.72	0.19	5.63	9.29	0.10	0.19	19.11	4.21	-0.14	-0.59	0.84	2.21	2.08	8.63	1.11	1.00	5.21	2.59	-0.39	6.47	9.29	2.31	2.27	27.73	1.15	1.45	9.29
ER	Ein Balsam	2016	0.811	0.515	0.381	1.378	0.434	0.144	2.151	5.816	0.94	2.56	0.18	5.29	8.73	0.09	0.17	17.96	4.25	-0.28	-0.26	-1.01	2.54	2.41	7.65	1.27	0.86	5.19	2.28	-0.07	4.27	8.73	2.63	2.58	25.62	1.31	1.28	8.73
ER	Ein Reach	2016	0.663	0.508	0.283	1.654	0.458	0.129	2.133	5.828	1.09	2.97	0.21	6.14	10.15	0.10	0.20	20.87	4.75	-0.44	-0.14	-0.84	2.43	2.44	8.21	1.22	1.16	5.84	2.54	0.08	5.30	10.15	2.54	2.64	29.08	1.27	1.65	10.15
ER	Ein Reach	2000	0.628	0.506	0.260	1.718	0.464	0.125	2.129	5.830	0.88	2.42	0.17	5.00	8.25	0.08	0.17	16.97	5.60	0.33	-0.12	-0.48	2.18	3.64	11.15	1.09	1.71	6.49	2.75	0.05	4.52	8.25	2.27	3.80	28.12	1.13	2.11	8.25
ER	Ein Reach	2004	0.800	0.515	0.374	1.400	0.436	0.143	2.150	5.817	1.00	2.73	0.19	5.64	9.31	0.10	0.19	19.15	4.92	0.01	-0.25	-0.24	2.25	3.46	10.14	1.12	1.34	5.92	2.74	-0.05	5.39	9.31	2.34	3.64	29.29	1.17	1.79	9.31
EM	Ein Makla	2016	0.926	0.522	0.457	1.166	0.416	0.156	2.165	5.807	1.39	3.80	0.27	7.86	12.98	0.13	0.26	26.70	5.18	-1.12	-0.29	0.10	2.84	1.15	7.87	1.42	1.17	6.57	2.69	-0.02	7.96	12.98	2.97	1.41	34.57	1.48	1.80	12.98
EM	Ein Makla	2000	0.765	0.513	0.351	1.463	0.442	0.139	2.146	5.820	1.43	3.91	0.28	8.07	13.33	0.14	0.27	27.41	6.72	-0.78	-0.17	-0.31	3.02	3.16	11.65	1.51	1.85	8.15	3.12	0.11	7.76	13.33	3.16	3.43	39.06	1.58	2.50	13.33
EM	Ein Makla	2004	0.765	0.513	0.351	1.463	0.442	0.139	2.146	5.820	1.36	3.72	0.27	7.68	12.69	0.13	0.25	26.10	5.46	-0.77	-0.17	-0.02	2.87	2.95	10.32	1.44	1.29	6.82	2.95	0.09	7.66	12.69	3.00	3.21	36.41	1.50	1.91	12.69
ME1	Meizar 1	2016	0.537	0.501	0.200	1.888	0.478	0.116	2.118	5.837	1.12	3.05	0.22	6.30	10.41	0.11	0.21	21.41	0.95	-2.15	-0.08	1.81	0.04	1.24	1.80	0.02	0.45	2.06	0.90	0.13	8.11	10.41	0.15	1.45	23.21	0.07	0.96	10.41
ME2	Meizar 2	2016	0.388	0.493	0.101	2.164	0.502	0.100	2.101	5.849	1.13	3.09	0.22	6.39	10.56	0.11	0.21	21.71	6.98	-0.54	0.29	0.57	6.83	1.31	15.45	3.42	0.07	8.11	2.55	0.51	6.97	10.56	6.94	1.52	37.16	3.47	0.59	10.56
ME2	Meizar 2	2001	0.388	0.493	0.101	2.164	0.502	0.100	2.101	5.849	0.90	2.47	0.18	5.10	8.43	0.09	0.17	17.34	5.83	-0.10	0.28	0.48	5.61	1.73	13.82	2.80	0.11	6.73	2.37	0.46	5.58	8.43	5.70	1.90	31.16	2.85	0.52	8.43
ME3	Meizar 3	2016	0.880	0.519	0.427	1.251	0.423	0.151	2.159	5.811	0.19	0.53	0.04	1.09	1.80	0.02	0.04	3.70	2.48	1.01	-0.36	-0.03	0.23	3.22	6.54	0.12	1.12	0.08	1.24	-0.29	1.88	1.63	0.19	1.80	6.52	0.09	-0.05	1.63
ME3	Meizar 3	2001	0.388	0.493	0.101	2.164	0.502	0.100	2.101	5.849	0.13	0.36	0.03	0.75	1.24	0.01	0.02	2.54	2.74	0.87	-0.01	-0.80	-0.03	3.04	5.81	-0.01	1.39	-1.66	0.70	0.08	1.40	0.94	-0.13	0.51	1.83	-0.07	-0.77	0.94
Estimates based on basaltic-rock-, Golan limestone water and Rish Pinna brine																																					
AS	Ain Saraya	2016	1.29	0.54	0.70	0.49	0.36	0.19	2.21	5.78	3.46	0.86	0.13	5.03	9.29	0.35	0.09	19.21	1.74	1.72	-0.52	1.44	1.96	2.18	8.52	0.98	-0.11	5.21	2.59	-0.39	6.47	9.29	2.31	2.27	27.73	1.15	1.45	9.29
ER	Ein Balsam	2016	0.81	0.52	0.38	1.38	0.43	0.14	2.15	5.82	3.26	0.81	0.12	4.73	8.73	0.33	0.08	18.06	1.93	1.47	-0.20	-0.45	2.30	2.50	7.55	1.15	-0.18	5.19	2.28	-0.07	4.27	8.73	2.63	2.58	25.62	1.31	1.28	8.73
ER	Ein Reach	2016	0.66	0.51	0.28	1.65	0.46	0.13	2.13	5.83	3.78	0.94	0.14	5.49	10.15	0.38	0.10	20.99	2.05	1.60	-0.07	-0.19	2.16	2.55	8.09	1.08	-0.05	5.84	2.54	0.08	5.30	10.15	2.54	2.64	29.08	1.27	1.65	10.15
ER	Ein Reach	2000	0.63	0.51	0.26	1.72	0.46	0.13	2.13	5.83	3.08	0.77	0.12	4.47	8.25	0.31	0.08	17.06	3.41	1.98	-0.07	0.05	1.96	3.72	11.06	0.98	0.73	6.49	2.75	0.05	4.52	8.25	2.27	3.80	28.12	1.13	2.11	8.25
ER	Ein Reach	2004	0.80	0.51	0.37	1.40	0.44	0.14	2.15	5.82	3.47	0.86	0.13	5.04	9.31	0.35	0.09	19.25	2.45	1.87	-0.18	0.35	1.99	3.56	10.04	1.00	0.23	5.92	2.74	-0.05	5.39	9.31	2.34	3.64	29.29	1.17	1.79	9.31
EM	Ein Makla	2016	0.93	0.52	0.46	1.17	0.42	0.16	2.16	5.81	4.84	1.20	0.19	7.03	12.98	0.49	0.12	26.85	1.73	1.48	-0.21	0.94	2.48	1.29	7.72	1.24	-0.37	6.57	2.69	-0.02	7.96	12.98	2.97	1.41	34.57	1.48	1.80	12.98
EM	Ein Makla	2000	0.77	0.51	0.35	1.46	0.44	0.14	2.15	5.82	4.97	1.24	0.19	7.21	13.33	0.50	0.13	27.57	3.18	1.89	-0.08	0.55	2.66	3.30	11.50	1.33	0.26	8.15	3.12	0.11	7.76	13.33	3.16	3.43	39.06	1.58	2.50	13.33
EM	Ein Makla	2004	0.77	0.51	0.35	1.46	0.44	0.14	2.15	5.82	4.73	1.18	0.18	6.87	12.69	0.48	0.12	26.24	2.09	1.77	-0.09	0.79	2.52	3.09	10.17	1.26	-0.22	6.82	2.95	0.09	7.66	12.69	3.00	3.21	36.41	1.50	1.91	12.69
ME1	Meizar 1	2016	0.537	0.501	0.200	1.888	0.478	0.116	2.118	5.837	3.88	0.97	0.15	5.64	10.41	0.39	0.10	21.53	-1.82	-0.07	-0.01	2.48	-0.24	1.35	1.68	-0.12	-0.79	2.06	0.90	0.13	8.11	10.41	0.15	1.45	23.21	0.07	0.96	10.41
ME2	Meizar 2	2016	0.388	0.493	0.101	2.164	0.502	0.100	2.101	5.849	3.94	0.98	0.15	5.71	10.56	0.40	0.10	21.83	4.18	1.57	0.36	1.25	6.54	1.42	15.33	3.27	-1.18	8.11	2.55	0.51	6.97	10.56	6.94	1.52	37.16	3.47	0.59	10.56
ME2	Meizar 2	2001	0.388	0.493	0.101	2.164	0.502	0.100	2.101	5.849	3.14	0.78	0.12	4.56	8.43	0.32	0.08	17.43	3.59	1.59	0.34	1.02	5.38	1.82	13.73	2.69	-0.90	6.73	2.37	0.46	5.58	8.43	5.70	1.90	31.16	2.85	0.52	8.43
ME3	Meizar 3	2016	0.880	0.519	0.427	1.251	0.423	0.151	2.159	5.811	0.67	0.17	0.03	0.97	1.80	0.07	0.02	3.72	2.00	1.37	-0.35	0.08	0.18	3.24	6.52	0.09	0.91	2.67	1.54	-0.33	1.05	1.80	0.25	3.25	10.24	0.13	1.21	1.80
ME3	Meizar 3	2001	0.388	0.493	0.101	2.164	0.502	0.100	2.101	5.849	0.46	0.11	0.02	0.67	1.24	0.05	0.01	2.56	2.42	1.11	0.00	-0.72	-0.06	3.06	5.80	-0.03	1.24	2.88	1.23	0.02	-0.06	1.24	-0.02	3.07	8.36	-0.01	1.45	1.24

References

1. Anders, E.; Grevesse, N. Abundance of elements: meteoric and solar. *Geochim Cosmochim Acta* **1989**, 53, 197–214.
2. Arad, A.; Bein, A. Saline- versus freshwater contribution to the thermal waters of the northern Jordan Rift Valley. *Isr J Hydrol* **1986**, *83*, 49–66.
3. Bajjali, W.; Clark, I.D.; Fritz, P. The artesian thermal groundwaters of northern Jordan: Insights into their recharge history and age. *J Hydrol* **1997**, *192*, 355–382.
4. Bau, M. Scavenging of dissolved yttrium and rare earths by precipitating iron oxyhydroxide: experimental evidence for Ce oxidation, Y–Ho fractionation, and lanthanide tetrad effect. *Geochim Cosmochim Acta* **1999**, *63*, 67–77.
5. Bergelson, G.; Nativ, R.; Bein, A. Salinization and dilution history of ground water discharging into the Sea of alilee, the Dead Sea Transform, Israel. *Appl Geochem* **1999**, *14*, 91–118.
6. Bevenisti, E.; Gvirtzman, H.; Harnessing international law to determine Israeli-Palestinian water rights: The mountain aquifer. *Nature Res J* **1993**, *33*, 543–567.
7. Clemens, M.; Khurelbaatar, G.; Merz, R.; Siebert, C.; van Affrden, M.; Rödiger. T. Groundwater protection under water scarcity; from regional risk assessment to local wastewater treatment solutions. *Sci Total Environment* **2020**, *706*, 136066. https://doi.org/10.1016/j.scitotenv.2019.136066.
8. Dafny, E.; Burg, A.; Gvirtzman, H. Deduction of groundwater flow regime in a basaltic aquifer using geochemical and isotopic data; The Golan Heights, Israel case study. *J Hydrol* **2006**, *330*, 506–524.
9. Etana Files. The Yarmouk Basin. Between conflict and development. Periodical Bulletin about Civil Society and Local Governance in Syria, **2015**, *11*, July 2015.
10. Flexer, A. Stratigraphy and facies development of Mount Scopus (Senonian-Paleocene) in Israel and adjacent countries.*Isr J Earth Sci* **1968**, *17*, 85–114.
11. Gilad, D.; Schwartz, S. Hydrogeology of the Jordan sources aquifers. *Isr Hydrol Serv Rep* (in Hebrew) Hydro **1978**, *5/78*, 58 pp.
12. Inbar, N.; Raggad, M.; Siebert, C.; Möller, P.; Rödiger, T.; Rosenthal, E.; Guttman, J.; Magri, F. Active tectonics at the Lower Yarmouk Gorge? *Geophys Res Abstract*, EGU Assembly Vienna 2017, **2017**, *19*, 9563.
13. Inbar, N.; Rosenthal, E.; Magri, F.; Alraggad, M.; Möller, P.; Flexer, A.; Guttman, J.; Siebert, C. Faulting patterns in the Lower Yarmouk Gorge potentially influence groundwater flow paths. *Hydrol Earth Syst Sci* **2019**, *23*, 763–771.
14. Johannesson, K.H.; Farnham, I.M.; Stetzenbach, K.J. Rare earth element fractionation and concentration variation along a groundwater flow path within shallow basin fill aquifer, southern Nevada, USA. *Geochim Cosmochim Acta* **1999**, *63*, 2697–2708.
15. Johannesson, K.H.; Tang, J.; Daniels, J.M.; Bounds, W.J.; Burdidge, D.J. Rare earth element concentrations and speciation in organic-rich blackwaters of the Great Dismal Swamp, Virginia, USA. *Chem Geol* **2004**, *209*, 271–294.
16. Johannesson, K.H.; Zhou, X.; Guo, C.; Stetzenbach, K.J.; Hodge, V.F. Origin of rare earth element signatures in ground water of circumneutral pH from Nevada and eastern California. *Chem Geol* **2000**, *164*, 239–257.
17. Kattan, Z. Chemical and environmental isotope study of the fissured basalt aquifer system of the Yarmouk basin. *IAEA Symposium on isotopes in water resources management.* Vienna, Austria. 1995, IAEA-SM/336/28.
18. Kattan, Z. Chemical and environmental isotope study of precipüitation in Syria. *J Arid Environ* **1997**, *36*, 601–615.
19. Klein BenDavid, O.; Sass, E.; Katz, A. The evolution of marine evaporitic brines in inland basins: The Jordan-Dead Sea Rift valley. *Geochim Cosmochim Acta* **2004**, *68*, 1763–1775.
20. Lawrence, M.G.; Jupiter, S.D.; Kamber, B.S. Aquatic geochemistry of rare earth elements and Yttrium in the Pioneer River catchment, Australia. *Mar Freshw Res* **2006**, *57*, 725–736.
21. Mandel, S. Chemical analyses in observation boreholes since 1950. Final report on the Lake Tiberias Salinity Committee, Tahal-Water Planning for Israel Ltd. (1965) vol. l1-3.
22. Maqqram, H. Hydrogeological study of water resources in the basin of Jebel Druz (Jebel el Arab). Syrian Arab Republic, Rep. Division for Water Resources (in Arabic) 1996.
23. McCaffrey, M.A.; Lazar, B.; Holland, H.D. The evaporation path of seawater and the coprecipitation of Br^- and K^+ with halite. *J Sediment Petrol* **1987**, *57*, 928–937.

24. Meiler M.; Reshef, H.; Shulman, H. Seismic depth domain stratigraphic classification of the Golan Heights, Central Dead Sea Fault. *Tectonophysics* **2011**, *510*, 354–369.
25. Michelson, H. The Geology and Paleogeography of the Golan Heights, Tel Aviv University, Tel Aviv, PhD thesis, **1979**, 163 pp.
26. Möller, P.; Siebert, C. Cycling of calcite and hydrous metal oxides and chemical changes of major element and REE chemistry in monomictic hardwater lake: Impact on sedimentation. *Chemie der Erde/Geochem* **2016a**, *76*, 133–148.
27. Möller, P.; Dulski, P.; Salameh, E.; Geyer, S. Characterization of the sources of thermal spring- and well water in Jordan by rare earth element and yttrium distribution and stable isotopes. *Acta Hydrochim Hydrobiol* **2006a**, *34*, 101–116.
28. Möller, P.; Geyer, S.; Salameh, E.; Dulski, P. Sources of mineralization and salinization of thermal groundwater of Jordan. *Acta Hydrochim Hydrobiol* **2006b**, *34*, 86–100.
29. Möller, P.; Rosenthal, E.; Dulki, P.; Geyer, S.; Guttman, Y. Rare earths and yttrium hydrostratigraphy along the Lake Kinneret-Dead Sea- Arava transform fault, Israel and adjoining territories. *Appl Geochem* **2003**, *18*, 1613–1628.
30. Möller, P.; Rosenthal, E.; Inbar, N.; Magri, F. Hydrochemical considerations for identifying water from basaltic aquifers: The Israeli experience. *J Hydrol: Regional Studies* **2016b**, *5*, 33–47.
31. Möller, P.; Rosenthal, E.; Inbar, N.; Siebert, C. Development of the Inland Sea and its evaporites in the Jordan-Dead Sea Transform based on hydrogeochemical considerations and the geological consequences. *Intern J Earth Sci* **2018**, *107*, 2409–2431.
32. Möller, P.; Siebert, C.; Geyer, S.; Inbar, N.; Rosenthal, E.; Flexer, A.; Zilberbrand, M. Relationship of brines in the Kinnarot basin, Jordan-Dead Sea Rift valley. *Geofluids* **2012**, *12*, 166–181.
33. Mor, D. The volcanism of the Golan Heights. *Geol Surv Isr Rep.GSI/5/86* (in Hebrew with extended English abstract) **1986**.
34. Olsson, J.; Stipp, S.L.S.; Makvichy, E.; Gislason, S.R. Metal scavenging by calcium carbonate at the Eyjafjallajökull volcano: A carbon capture and storage analogue. *Chem Geol* **2014**, *384*, 135–148.
35. Quinn, K.A.; Byrne, R.H.; Schijf, J. Comparative scavenging of yttrium and the rare earth elements in seawater: Compatitive influence of solution and surface chemistry. *Aquat Geochem* **2004**, *10*, 59–80.
36. Qura'an, A. The gravitational studies of the north-western part of Jordan. MSc Thesis Amman, University of Jordan **1991**.
37. Raab, M. The origin of the evaporites in the Jordan-Arava valley in view of the evolution of brines and evaporites during seawater evaporation. PhD thesis The Hebrew University of Jerusalem (in Hebrew) **1996**, 114 pp.
38. Reynolds, A.; Richards, G.; de la Iglesia, B.; Rayward-Smith, V. Clustering rules: A comparison of partitioning and hierarchical clustering algorithms. *J Math Model Algorithms* **1992**, *5*, 475–504.
39. Roded, R.; Shalev, E.; Katoshevski, D. Basalt Heat flow and hydrothermal regime at the Golan-Ajloun hydrological basins. *J Hydrol* **2013**, *476*, 200–211.
40. Rödiger, T.; Geyer, S.; Mallast, U.; Merz, R.; Krause, P.; Siebert, C. Multi-response calibration of a conceptual hydrological model in the semiarid catchment of Wadi al Arab, Jordan. *J Hydrol* **2014**, *509*, 193–206.
41. Rosenthal, E. Hydrogeology and Hydrogeochemistry of the Bet Shean and Harod Valleys. Geol Surv Israel, Rep. **1972**, H/2/1972, in Hebrew, 2 vols.
42. Rosenthal, E.; Möller, P.; Buch-Leviatan, O.; Politi, M. The hydrogeochemical stratigraphy of groundwater and its implications on water management in the central Jordan-Dead Sea Rift Valley, Israel. *Geofluids* (under review).
43. Rosenthal, E.; Möller, P.; Siebert, C.; Magri, F.; Guttman, J.;Inbar, N. Hydrology, hydrogeology and hydrogeochemistry of the Yarmouk basin. *Environ Earth Sci* **2020**, *79*, 71; https://doi.org/10.1007/s12665-019-8792-0.
44. Rosenthal, E.; Weinberger, G.; Almogi-Labin, A.; Flexer, A. Late Cretaceous – Early Tertiary development of depositional basins in Samaria (Israel) as part of the evolution of regional folding systems. *AAPG Bull* **1999**, *84*, 997–1042.
45. Sahawneh, J. Structural control of hydrology, hydrogeology and hydrochemistry along the eastern escarpment of the Jordan Rift Valley, Jordan. PhD Thesis, Karlsruher Inst. für Technologie (KIT), **2011**, 284 pp.

46. Salameh, E. Using environmental isotopes in the study of recharge-discharge mechanisms of the Yarmouk catchment area in Jordan. *Hydrogeol J* **2004**, *12*, 451–463.
47. Salameh, E.; Bannayan, H. Water Resources of Jordan - present status and future Potentials. Friedrich Ebert Stiftung (FES) and Royal Society for the Conservation of Nature (RSCN), Amman **1996**, 178 pp.
48. Sener, M.F.; Sener, M.; Uysal, T. The evolution of the Cappadocia geothermal province, Anatolia, (Turkey): geochemical and geochronological evidence *Hydrogeol J* **2017**, *25*, 2323–2345.
49. Shimron, A.E. Geochemical exploration and new geological data along the SE flanks of the Hermon Range, *Geol Surv Isr, Jerusalem* **1989**, Rep GSI/32/89.
50. Siebert, C.; Geyer, S.; Möller, P.; Rosenthal, E.; Berger, D.; Guttman, J. Lake Tiberias and its dynamic hydrochemical environment; in *The water of the Jordan Valley*, Hoetzel, H.; Möller, P.; Rosenthal, E., Eds.; Springer Berlin Heidelberg, Germany, **2009**, 219–246.
51. Siebert, C.; Möller, P.; Geyer, S.; Kraushaar, S.; Dulski, P.; Guttman, J.; Suhah, A.; Rödiger, T. Thermal waters in the Lower Yarmouk Gorge and their relation to surrounding aquifers. *Chemie der Erde/Geochem* **2014**, *74*, 425–441.
52. Siebert, C.; Möller, P.; Magri, F.; Shaliv, E.; Rosenthal, E.; Al-Raggad, M.; Rödiger, T. Applying rare earth elements, uranium and $^{87}Sr/^{86}Sr$ to disentangle structurally enforced confluence of regional groundwater resources, the case of the Lower Yarmouk Gorge. *Geofluids* **2019**, https://doi.org/101155/2019/6727681.
53. Siebert, C.; Rosenthal, E.; Möller, P.; Rödiger, T.; Meiler, M. The hydrochemical identification of groundwater flowing to the Bet She'an–Harod multiaquifer system (Lower Jordan Valley) by rare earth elements, yttrium, stable isotopes (H, O) and Tritium. *Appl Geochem* **2012**, *27*, 703–714.
54. Starinski, A. Relationship between Ca-chloride brines and sedimentary rocks in Israel. PhD thesis, Hebrew University, Jerusalem (in Hebrew, English summary) **1974**.
55. Stipp, S.L.S.; Cristensen, J.T.; Lakstanov, L.Z.; Baker, J.A.; Waight, T.E. Rare earth element (REE) incorporation in natural calcite: Upper limits for actinide uptake in a secondary phase. *Radiochim Acta* **2006**, *94*, 523–528.
56. Tanaka, K.; Miura, N.; Asahara, Y.; Kawabe, I. Rare earth element and strontium isotopic study of seamount-type limestone in Mesozoic accretionary complex of southern Chichibu Terrane, central Japan: Implication for incorporation process of seawater REE into limestones. *Geochem J* **2003**, *37*, 163–180.
57. Tanaka, K.; Kawabe, I. REE abundance in ancient seawater inferred from marine limestones and experimental REE partition coefficients between calcite and aqueous solution. *Geochem J* **2006**, *40*, 425–435.
58. Tanaka, K.; Ohta, A.; Kawabe, I. Experimental REE partitioning between calcite and aqueous solutions at 25 °C and 1 atm: Constraints on the incorporation of seawater REE into seamount-type limestones. *Geochem J* **2004**, *38*, 19–32.
59. Terakado, Y.; Masuda, A. The coprecipitation of rare-earth elements with calcite and aragonite. *Chem Geol* **1988**, *69*, 103–110.
60. Toyama, K.; Terakado, Y. Experimental study of rare earth element partitioning between calcite and sodium chloride solution at room temperature and pressure. *Geochem J* **2014**, *48*, 463–477.
61. Tzoufka, K.; Magri, F.; Rödiger, T.; Inbar, N.; Shalev, E.; Möller, P.; Raggad, M.; Rosenthal, E.; Siebert, C. *Hydrol J* **2018**, doi.org/10.1007/s10040-018-1827-x.
62. Wood, W.W. Geogenic groundwater solutes: the myth. *Hydrogeol J* **2019**, 27, 2729–2738, https://doi.org/10.1007/s10040-019-025057-1.